The Geodynamic Implications of Passive Margin Subduction in Northwest Turkey

C F Campbell, M A Mueller, M H Taylor, F Ocakoğlu, A Möller, G Métais, P M C Coster, K C Beard, Alexis Licht

Geochemistry, Geophysics, Geosystems®

AGU ADVANCING EARTH AND SPACE SCIENCE

RESEARCH ARTICLE
10.1029/2022GC010481

Special Section:
Tethyan dynamics: from rifting to collision

The Geodynamic Implications of Passive Margin Subduction in Northwest Turkey

C. F. Campbell[1], M. A. Mueller[2,3], M. H. Taylor[1], F. Ocakoğlu[4], A. Möller[1], G. Métais[5], P. M. C. Coster[6], K. C. Beard[7,8], and A. Licht[2,9]

[1]Department of Geology, University of Kansas, Lawrence, KS, USA, [2]Department of Earth and Space Sciences, University of Washington, Seattle, WA, USA, [3]Department of Geosciences, University of Connecticut, Storrs, CT, USA, [4]Department of Geological Engineering, Eskişehir Osmangazi University, Eskişehir, Turkey, [5]Centre de Recherches sur la Paléobiodiversité et les Paléoenvironnements, Muséum National d'Histoire Naturelle, Paris, France, [6]Réserve Naturelle Nationale Géologique du Luberon, Apt, France, [7]Biodiversity Institute, University of Kansas, Lawrence, KS, USA, [8]Department of Ecology and Evolutionary Biology, University of Kansas, Lawrence, KS, USA, [9]CNRS, IRD, INRAE, Collège de France, CEREGE, Aix-Marseille Université, Aix-en-Provence, France

Abstract The number of subduction zones that facilitated the northward translation of the Anatolide-Tauride continental terrane derived from Gondwana to the southern margin of Eurasia at the longitude of western Turkey is debated. We hypothesized that if two north dipping subduction zones facilitated incipient collision in western Turkey, a late Cretaceous arc would have formed within the Neotethys and along the southern margin of Eurasia. To determine if an island arc formed within the Neotethys we investigated the sedimentary record of the Central Sakarya basin, which was deposited along the southern margin of Eurasia from 85 to 45 million years ago. Detrital zircon deposited within the lower levels of the Central Sakarya basin (the Değirmenözü Formation) are associated with south to north-directed paleocurrents and exhibit a unimodal late Cretaceous age peak sourced from isotopically juvenile mantle melts. Zircon maximum depositional ages from the Değirmenözü Formation cluster between 95 and 90 Ma and are 5–10 Myr older than biostratigraphic depositional ages. Between 95 and 80 Ma, a 12-unit shift from mantle to crustal derived εHf values occurs in the overlying Yenipazar Formation. We explain the absence of Paleozoic, Eurasian-sourced detrital zircon, the rapid shift from mantle to crustal derived εHf values, and lag time in terms of passive margin subduction within an isolated intra-oceanic subduction zone, whose island arc was reworked from south to north into the Central Sakarya basin during incipient collision. Thus, widely outcropping late Cretaceous plutonic rocks within Eurasia must have belonged to an additional convergent margin.

Key Points:

- We leveraged the isotopic signature of subducted passive margin to test incipient collision models in northwest Turkey
- Passive margin subduction resulted in the development of an isolated intra-oceanic basin
- Two north dipping subduction zones facilitated incipient collision in the region

Supporting Information:

Supporting Information may be found in the online version of this article.

Correspondence to:

C. F. Campbell,
clayc@ku.edu

Citation:

Campbell, C. F., Mueller, M. A., Taylor, M. H., Ocakoğlu, F., Möller, A., Métais, G., et al. (2023). The geodynamic implications of passive margin subduction in northwest Turkey. *Geochemistry, Geophysics, Geosystems*, *24*, e2022GC010481. https://doi.org/10.1029/2022GC010481

Received 13 APR 2022
Accepted 10 DEC 2022

Author Contributions:

Conceptualization: M. A. Mueller, M. H. Taylor, F. Ocakoğlu, G. Métais, P. M. C. Coster, K. C. Beard, A. Licht
Formal analysis: M. A. Mueller, M. H. Taylor, A. Möller
Funding acquisition: M. H. Taylor, K. C. Beard

1. Introduction

The Alpine-Himalaya orogenic system extends from Western Europe to Indonesia (e.g., Şengör, 1987) and is the result of collisions between rifted continental slivers derived from the northern margin of Gondwana with the southern margin of Eurasia beginning in late Mesozoic–mid Cenozoic times (e.g., Ballato et al., 2011; Cowgill et al., 2016; Darin et al., 2018; Kapp & DeCelles, 2019; McQuarrie et al., 2003; Okay et al., 2010; Robertson & Dixon, 1984; Şengör & Yilmaz, 1981; Yin & Harrison, 2000). A growing body of geologic, paleomagnetic and geochemical evidence (e.g., Aitchison et al., 2000; Bouilhol et al., 2013; Gnos et al., 1997; Hall, 2012; van Hinsbergen et al., 2016, 2020; Westerweel et al., 2019) indicates that the northward translation of such terranes was accommodated by north dipping subduction zones located along the southern margin of Eurasia and within the Neotethyan Ocean (i.e., the Trans-Tethyan subduction zone; Jagoutz et al., 2015).

In Turkey (Anatolia), the Anadolu plate (Gürer et al., 2016) separated the northern Pontide terrane (Eurasia) from the southern Anatolide-Tauride Block (Gondwana) in late Cretaceous times along north dipping subduction zones within the İzmir-Ankara (Neotethyan) Ocean and along the southern margin of the Pontides. Importantly however, the western termination of the Anadolu plate, and thus the triple junction demarcating the termination of the north dipping double subduction zone system, is poorly constrained. Kinematic (Gülyüz et al., 2019; van Hinsbergen et al., 2016, 2020) and geochemical (e.g., Collins & Robertson, 1997, 1998; Dilek et al., 1999; van Yalınız & Göncüoğlu, 1998; Yaliniz et al., 1996, 2000) data from N-MORB (normal mid-ocean ridge basalt) and P-MORB (plume mid-ocean ridge basalt) ophiolite along the İzmir-Ankara suture zone as well as SSZ (supra-subduction zone) ophiolite along the Anatolide-Tauride Block indicate that this triple junction was located at least as far west as the Kirşehır Block in Central Anatolia (Kaymakçı et al., 2009; van Hinsbergen et al., 2016) and associated

Investigation: M. A. Mueller, F. Ocakoğlu, G. Métais, P. M. C. Coster, K. C. Beard, A. Licht
Methodology: F. Ocakoğlu
Supervision: M. H. Taylor, F. Ocakoğlu, A. Möller
Writing – original draft: M. H. Taylor
Writing – review & editing: M. A. Mueller, M. H. Taylor, F. Ocakoğlu, A. Möller, A. Licht

with ~750 km of intra-oceanic extension in Albian–Cenomanian times (van Hinsbergen et al., 2020). In contrast, only the supra-subduction zone ophiolite (associated with ~750 km of intra-oceanic extension) at and west of the longitude of the Central Sakarya basin has been identified within the İzmir-Ankara suture zone and throughout the Anatolide-Tauride Block (e.g., Collins & Robertson, 1997, 1998)—more consistent with flat slab subduction along a single intra-oceanic convergent margin (e.g., Okay et al., 2020).

Thus, the single and double subduction zone models have contrasting and testable predictions. If a single subduction zone accommodated incipient collision west of the Kirşehır Block (Figure 1; KB), in order for late Cretaceous plutonic rocks significant of arc volcanism in Pontides to be connected to the Trans-Tethyan intra-oceanic convergent margin the ~750 km of late Cretaceous supra-subduction extension must have been immediately followed by flat-slab subduction in Western Anatolia. However, if instead such plutonic rocks were connected to a subduction zone along the southern margin of Eurasia, the Trans-Tethyan intra-oceanic subduction zone would have likely been associated with an additional intra-oceanic arc during the closure of the İzmir-Ankara Ocean. Accordingly, if such an intra-oceanic basin formed between the Western Pontides and Anatolide-Tauride Block and was subsequently reworked into Central Sakarya basin, we would expect to observe significantly older detrital zircon maximum depositional ages with respect to biostratigraphic ages (i.e., lag time), the absence of Devonian and Carboniferous detrital zircon age populations significant of previously exhumed regions of the Pontide basement, and Hf isotopes in zircon reflecting subduction and partial melting of the Anatolide-Tauride Block passive margin. In this article, after we determine if one or two subduction zones facilitated incipient collision in late Cretaceous times, we contextualize the tectonic evolution of the broader region in terms of our preferred geodynamic setting.

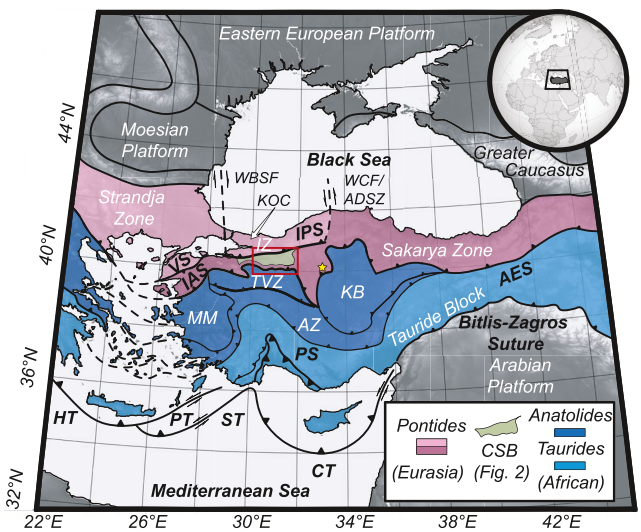

Figure 1. Terrane map of Greater Anatolia. The red polygon represents our general study area. The green polygon signifies the location of our main study area—the Central Sakarya basin (CSB). Thick lines represent suture/subduction zones and thinner lines represent major thrust sheets, where the barbs demarcate the hanging wall. The pink polygons represent the Eurasian affinity Pontides, which include: the Strandja Zone, İstanbul Zone (IZ), and Sakarya Zone. Major suture zones within the Pontides include the Vardar-Intra-Pontide suture (VS-IPS). Major north striking high angle structures in the Pontides include the dextral West Black Sea Fault (WBSF) and sinistral West Crimean Fault (WCF)/Araç-Daday shear zone (ADSZ). In contrast, the dark blue polygons represent the Anatolides, which include: the Tavşanlı Zone (TVZ), Afyon Zone (AZ), the Kirşehır Block (KB), and Menderes Massif (MM). Major suture zones within and to the south of the Anatolide-Tauride Block include the Pamphylian suture (PS) and Bitlis-Zagros suture. The İzmir-Ankara-Erzincan suture (IAS-AES) demarcates the contact between the Pontides and the Anatolide-Tauride Block. The location of present-day subduction is demarcated by the Hellenic Trench (HT), Pliny Trench (PT), Strabo Trench (ST), and Cyprus Trench (CT). Kocaeli Basin (KOC). The yellow star signifies the location of Ankara. Modified from Göncüoğlu et al. (2014), Hayward (1984), and Okay and Tüysüz (1999).

2. Geologic Background

The Strandja and İstanbul Zone (IZ) are located between the Black Sea back-arc basin and the Vardar- (VS) Intra-Pontide (IPS) suture zone. The Sakarya Zone is located south and east of the Vardar-Intra-Pontide suture zone and bound along its southern margin by the Neotethyan, İzmir-Ankara-Erzincan suture zone (IAS-AES). Together, the Strandja Zone, İstanbul Zone, and Sakarya Zone exhibit a post Silurian Eurasian (northern) affinity and are collectively known as the Turkish Pontides (Figure 1; e.g., Ketin, 1966; Okay & Tüysüz, 1999; Okay et al., 2002; Rolland et al., 2012; Şengör & Yilmaz, 1981). In contrast, the Menderes Massif (MM), Tavşanlı Zone (TVZ), Afyon Zone (AZ), and Kirşehır Block (KB) are located south of the İzmir-Ankara-Erzincan suture zone and were derived from the northern margin of Gondwana in post-Silurian times (e.g., Ketin, 1966; Okay & Tüysüz, 1999; Şengör & Yilmaz, 1981). Collectively, these terranes are known as the Anatolides (Figure 1), which exhibit significant yet contrasting metamorphic histories (e.g., Okay & Kelley, 1994; Pourteau et al., 2019; van Hinsbergen et al., 2016). We note that the Anatolides may not have been a single coherent terrane prior to late Cretaceous times (e.g., Pourteau et al., 2010). The Tauride Block is the southernmost terrane in Anatolia and is often interpreted as the unmetamorphosed equivalent of the Anatolides (e.g., Ketin, 1966). It has also been hypothesized that the Taurides and Anatolides were separate terranes prior to late Cretaceous times (e.g., Gülyüz et al., 2019; Moix et al., 2008; Speciale et al., 2012). The Anatolides and Taurides are commonly referred to as the Anatolide-Tauride Block (e.g., Şengör & Yilmaz, 1981), which is the term we adopt in this article. The Anatolide-Tauride Block and Pontides are juxtaposed along the İzmir-Ankara-Erzincan suture zone, which represents the location where a westward narrowing, oceanic embayment between Eurasia and Gondwana, known as the Neotethys closed (e.g., Okay & Tüysüz, 1999; Şengör & Yilmaz, 1981; Stampfli, 2000; Stampfli & Hochard, 2009; Stampfli et al., 2002). Below we review the tectonostratigraphy of the Tavşanlı Zone.

2.1. The Tavşanlı Zone

The Tavşanlı Zone (Okay, 1984) is defined by a 2–3 km thick, ∼250 km E–W by ∼50 km N–S belt (Kaya et al., 2001; Okay, 1980a, 1980b, 2002; Okay & Kelley, 1994; Okay & Whitney, 2010) of metamorphosed Carboniferous (Okay et al., 2008) and Triassic (Kaya et al., 2001) continental affinity sedimentary rocks known as the Orhaneli blueschist sequence. This succession of metamorphic rocks was subject to high pressure-low temperature (HP-LT) metamorphic conditions corresponding to 21–22 kbar and ∼425°C (Okay, 2002; Okay & Kelley, 1994; Pourteau et al., 2019) between 90 and 80 Ma (Mulcahy et al., 2014; Okay, 2002; Okay & Kelley, 1994; Okay et al., 1998; Plunder et al., 2015; Pourteau et al., 2019; Seaton et al., 2009, 2014; Sherlock & Kelley, 2002; Sherlock et al., 1999). Structurally above the Orhaneli blueschist is a sequence of ophiolitic mélange (Göncüoğlu et al., 2006, 2010) that was obducted above the Anatolides around 93 Ma, at *P-T* conditions corresponding to ∼17 kb and ∼650°C (Pourteau et al., 2019; van Hinsbergen et al., 2016). Finally, the metamorphic sole of overlying ophiolitic mélange formed at *P-T* conditions of 6–7 kb and 800–850°C around 104 Ma (Pourteau et al., 2019), during supra-subduction zone extension above the Trans-Tethyan intra-oceanic subduction zone (e.g., Göncüoğlu et al., 2006, 2010; Manav et al., 2004; Önen, 2003; Sarıfakıoğlu et al., 2009, 2010, 2017). Together, these three units represent the subducted and exhumed passive margin of the Anatolide-Tauride Block, overlying accretionary prism, and obducted oceanic crust, respectively (e.g., Okay, 1980a, 1980b, 1982, 1986; Kaya, 1972; Lisenbee, 1972; Plunder et al., 2013, 2015; Rojay, 2013; Rojay et al., 2004; Sarıfakıoğlu et al., 2014; Topuz et al., 2006; van der Kaaden, 1966).

3. Sedimentology and Stratigraphy of the Central Sakarya Basin

The Central Sakarya basin is characterized by a 5 km thick by 7,500 km^2 succession of Mesozoic and Cenozoic sedimentary and volcanic rocks deposited along the Sakarya Zone. The Central Sakarya basin is located south of the Intra-Pontide suture zone, north of the İzmir-Ankara suture zone, east of the longitude of Bursa (∼29°E), and west of the Galatean volcanic complex (∼32°E) (Figure 2; Altıner et al., 1991; Göncüoğlu et al., 2000; Ocakoğlu et al., 2018; Okay et al., 2001; Yilmaz et al., 2016). In the following section we define simplified map units (Figure 2), based on sections measured by Ocakoğlu et al. (2018), Mueller et al. (2019), and 1:100,000 geologic maps provided by the General Directorate of (Turkish) Mineral Exploration and Research (MTA; Akbaş et al., 2011; Aksay et al., 2002).

3.1. Devonian–Triassic Basement (DT)

The Sakarya Zone is characterized by metamorphosed Devonian passive margin strata intruded by Carboniferous and Permian granitoids (Kaygusuz et al., 2012; Okay et al., 1996; Okay, Satir, & Siebel, 2006; Okay & Whitney, 2010; Topuz et al., 2007, 2010, 2020; T. Ustaömer et al., 2013; Yilmaz et al., 2000). The Karakaya Complex is structurally below the metamorphosed Devonian passive margin strata and consists of a ∼3 km thick package of mafic metasedimentary rocks and Upper Triassic, Norian limestone blocks (Okay, 2000; Okay & Göncüoğlu, 2004; Okay et al., 2002; Pickett & Robertson, 2004; Tekin et al., 2002; Topuz et al., 2018; T. Ustaömer et al., 2016).

3.2. The Jurassic–Lower Cretaceous Basin Fill (JLK)

The Jurassic–Lower Cretaceous basin fill unconformably overlies the basement of the Sakarya Zone (Figure 3). This unit consists of carbonates and mafic volcanogenic layers composed of beige-pink pelagic and reefal limestones. In turn, the carbonates and mafic volcanogenic layers interfinger with deeper marine, ammonite-bearing pelagic carbonates and calciturbidites containing clasts of chert nodules and olistoliths. Together, these sedimentary successions are known as the Bilecik Formation and the Soğukçam Limestone (Altıner et al., 1991). The Bilecik Formation and the Soğukçam Limestone are interpreted to reflect the growth and subsequent breakup of a carbonate platform during extensional tectonics in middle Jurassic–early Cretaceous times (Altıner et al., 1991).

3.3. The Upper Cretaceous–Middle Paleocene Basin Fill (UKMP)

The Upper Cretaceous units overlie the Jurassic–Lower Cretaceous section along an erosional surface (Altıner et al., 1991). The Değirmenözü Formation was deposited in Santonian times and consists of poorly sorted, angular pebble to boulder conglomeratic and volcanogenic slumps overlain by thinly bedded calciturbidites

10.1029/2022GC010481

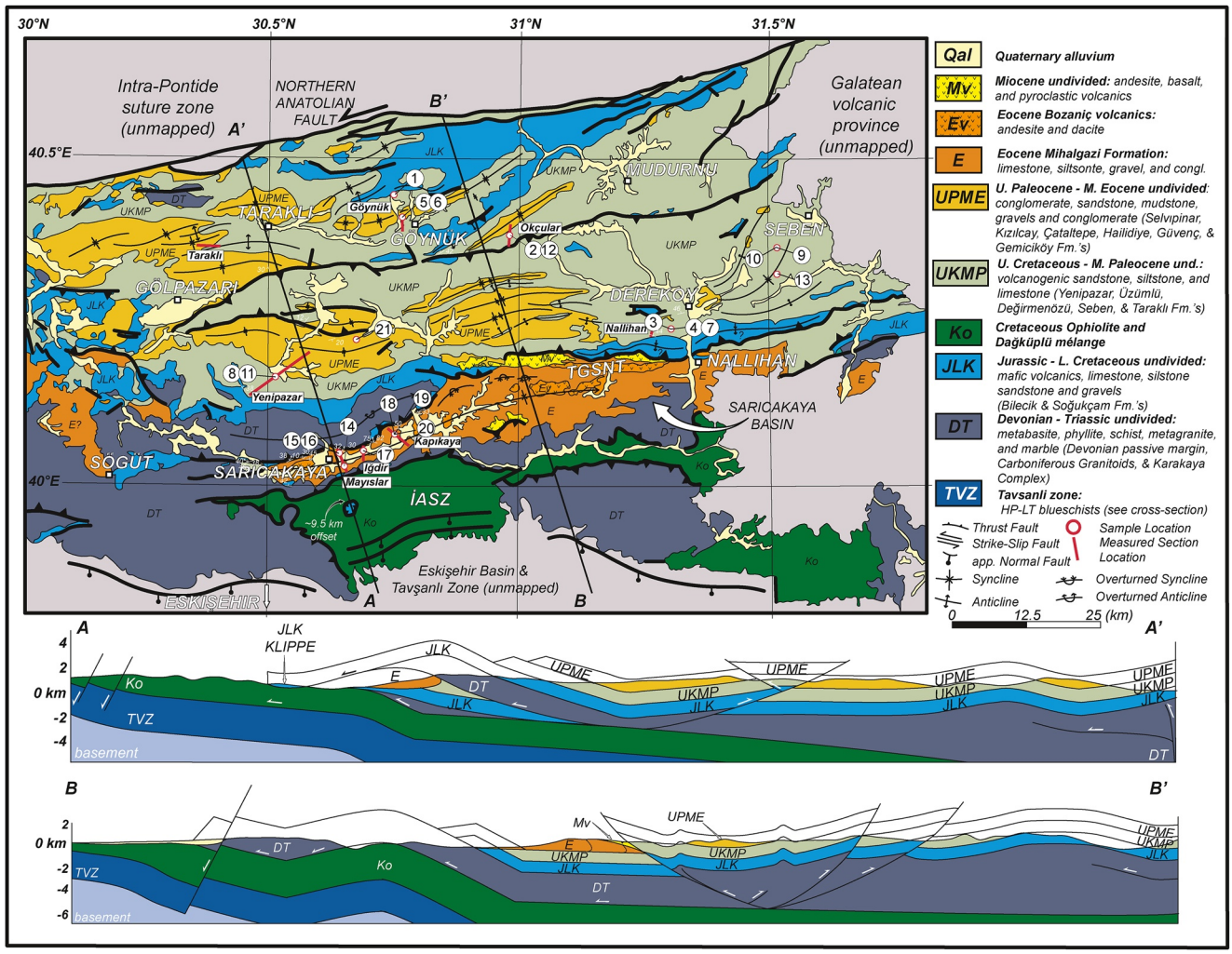

Figure 2. Simplified geologic map of the Central Sakarya basin (modified and compiled from Aksay et al. (2002), Okay et al. (2002), and Akbaş et al. (2011)). Detailed explanations of the map units can be found in Section 3 and the locations of previously measured stratigraphic sections in Ocakoğlu et al. (2018) and Mueller et al. (2019). Thick black lines without symbology represent high angle faulting. İzmir-Ankara suture zone (IASZ); Tuzaklı-Gümele-Söğüt-Nallıhan Thrust (TGSNT). Cross-sections exhibit minimal vertical exaggeration and are meant to illustrate the general structure of the Central Sakarya Basin. See Table 1 for sample information.

(Ocakoğlu et al., 2018; Wolfgring et al., 2017). The overlying Yenipazar Formation was deposited Campanian times where a demonstrable transition to siliceous, volcaniclastic turbidites, and pelagic mudstones is observed (Demirkol, 1977; Ocakoğlu et al., 2018 and references therein). Together the Değirmenözü and Yenipazar Formations exhibit south, southwest, southeast, east, and to a lesser extent east-northeast paleocurrents (Ocakoğlu et al., 2018; Figure 3). Fossils belonging to the Yenipazar and Değirmenözü Formations include: *Dicarinella asymetrica, Globotruncana elevata, Globotruncana ventricose, Globotruncana havanensis, Globotruncana aegytptiaca, Gansserina gansseri, Racemiguembelina fructicosa, Parasubbotina psuedobulloides,* and *Praemurica uncinata*. This indicates the Değirmenözü and Yenipazar Formations were deposited in late Santonian through Danian times (84.8–61.6 Ma; Ocakoğlu et al., 2018). The overlying Seben Formation was deposited in Maastrichtian times (72.1–66.0 Ma; Ocakoğlu et al., 2018) and is characterized by monotonous gray mudstones, yielding *Micula mura* along with various other nanofossils, bivalves and gastropods indicative of a shallow marine environment. Together the Upper Cretaceous–Middle Paleocene (UKMP) units are interpreted to represent the development and deepening of a volcanogenic, submarine basin shortly after Santonian times (Ocakoğlu et al., 2018; Wolfgring et al., 2017). A regional decrease in sea level occurred in mid-Campanian times. Following this drop, a shallow marine environment developed in Maastrichtian times and is recorded by a shoaling event (Ocakoğlu et al., 2018). Shoaling to a shallow marine environment was coeval with the onset of basement exhumation and continued uplift of the accretionary prism (Mueller et al., 2022).

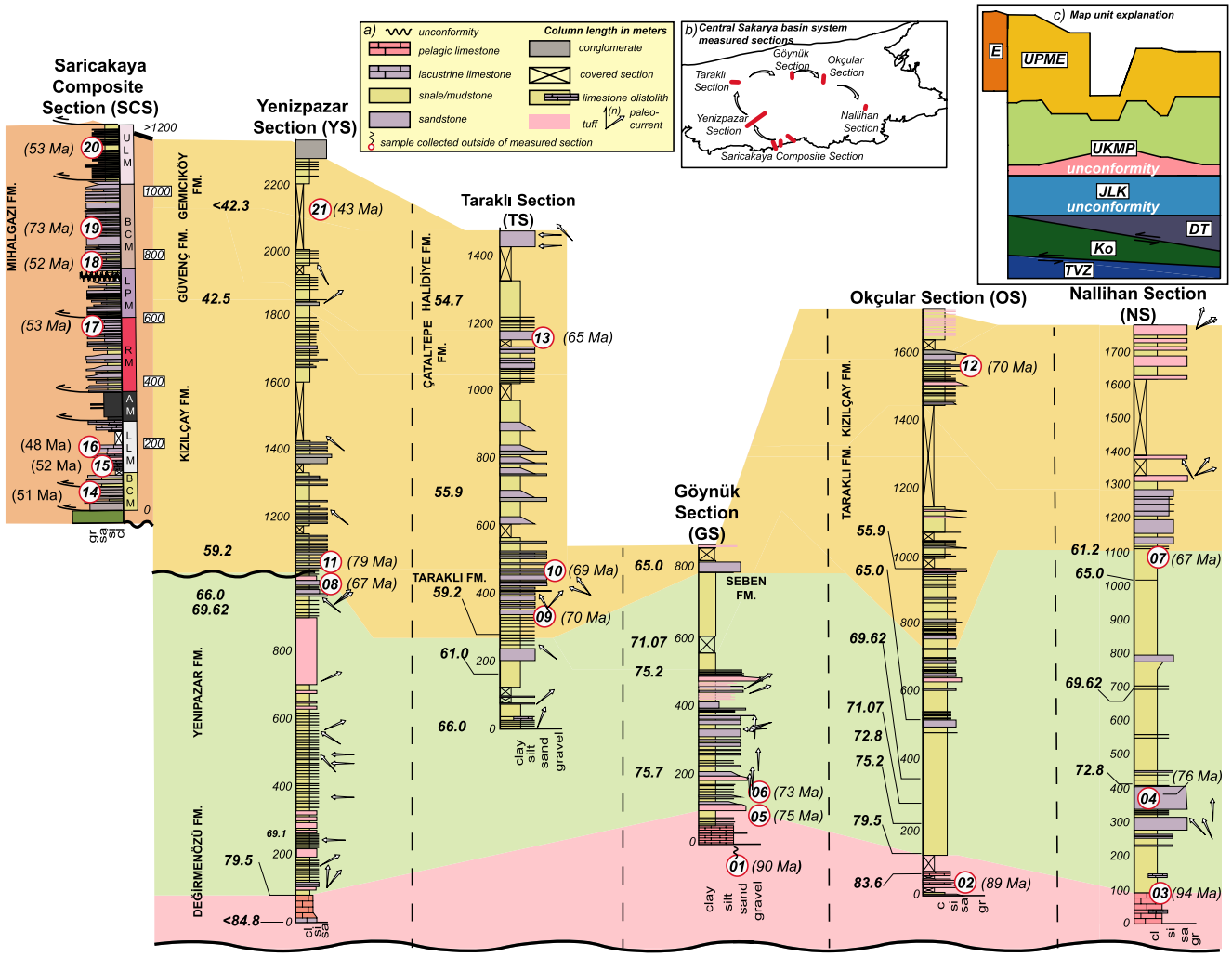

Figure 3. Simplified stratigraphic correlation used to constrain the relative ages of zircon U-Pb samples (circled numbers, see Figure 2 and Table 1) based on pre-existing biostratigraphy (bold numbers) and approximate zircon maximum depositional ages. (a) Key to interpreting the various stratigraphic columns. (b) Locations of measured sections relative to one another (also see Figure 2). (c) Simplified tectonostratigraphy of map units described in Section 3. Modified from Ocakoğlu et al. (2018) and Mueller et al. (2019).

3.4. The Upper Paleocene Through Middle Eocene Basin Fill (UPME)

Thick, fossiliferous, cross-bedded sandstones containing *Morozovella angulata* indicate the Taraklı Formation reflects continued shoaling to a deltaic environment in Selandian times (61.0–59.2 Ma; Ocakoğlu et al., 2018). In turn, the interfingering Kızılçay Formation describes the deposition of siliciclastic conglomerates and imbricated gravels which reflect a fluvial environment in Paleocene times (based on the presence of *Morozovelloides Lehneri*; 66.0–55.9 Ma; Kasapoğlu et al., 2016; Ocakoğlu et al., 2018; Şahin et al., 2019). Alternating mudstones, carbonate-shales, mollusks, corals, turbidites, hemipelagic muds, and fossiliferous limestones signal a rapid deepening event in the stratigraphically higher Çataltepe, Halidiye, Güvenç, and Gemiciköy Formations (Ocakoğlu et al., 2018 and references therein). The presence of *Morozovelloides lehneri* indicates these formations are as young as 42.3 Ma.

3.5. The Eocene Basin-Fill (E)

The Eocene Mihalgazi Formation describes a ∼1.5 km thick section of predominantly terrestrial strata within the Sarıcakaya basin (Figures 2 and 3; Mueller et al., 2019; Şahin et al., 2019; Okay et al., 2020). The Mihalgazi Formation was deposited prior to 51 Ma and after 47 Ma. It occurs as two ∼750 m thick fining-upward

sequences separated along an erosional surface. Importantly, the lower fining-upward sequence exhibits clasts of angular serpentinite, chert, and greenschists recording the northward progradation of alluvial fans derived from the İzmir-Ankara suture zone. In turn, the overlying fining-upward sequence consists of a basal conglomerate with clasts of serpentinite, chert, greenschist, gneiss, schist, and quartz clasts derived from both the İzmir-Ankara suture zone and the Sakarya Zone basement to the north. Contact metamorphic halos surround Middle Eocene andesite and dacite volcanic plugs, as part of the Bozaniç volcanic rocks (Ev). This indicates magmatism in the area post-dates deposition of the Mihalgazi Formation (e.g., Mueller et al., 2019). Finally, the Gemiciköy Formation consists of coarse-grained sandstones interpreted as the onset of fluvial deposition after 42.3 Ma (Ocakoğlu et al., 2018).

4. Hf Analytical Procedures

We refer the reader to Mueller et al. (2019, 2022) for U-Pb methods and data. All zircon U-Pb samples were analyzed for Hf isotopes at The University of Arizona LaserChron Center. Cathodoluminescence (CL) images ensured that 40 μm diameter Hf spots were placed above U-Pb pits that only ablated a zircon core or rim. Measurement precision for individual analyses are expressed using 2 s average uncertainty (±~3 εHf units). We collected Hf data for isotopic fingerprinting from 21 late Cretaceous–Eocene sedimentary and extrusive volcaniclastic rock zircon samples (Mueller et al., 2022; Ocakoğlu et al., 2018). Hafnium (Hf) isotopes were analyzed from 508 individual zircon with ages between 120 and 40 Ma. Generally, ~10 unknowns were analyzed for each age peak according to Gehrels and Pecha (2014).

$^{176}Hf/^{177}Hf$ ratios are especially useful for isotopic fingerprinting as Lutetium (Lu) has a relatively small atomic radius and preferentially partitions into residual mineral melt phases such as garnet. Through a Beta particle ejection, ^{176}Lu decays to ^{176}Hf with a half-life of approximately 37.2 Gyr (Scherer et al., 2001; Söderlund et al., 2004). Therefore, over geologic time, Earth's mantle has preferentially accumulated ^{176}Lu relative to crustal domains, and thus through radioactive decay, the mantle has also been preferentially enriched with ^{176}Hf. Hafnium has an atomic radius very similar to that of Zirconium and thus substitutes into zircon crystals on the order of parts per 10,000. In contrast, Lutetium is generally incompatible in the zircon crystal lattice. Therefore, the $^{176}Hf/^{177}Hf$ ratio in zircon fingerprints the host melt, with negligible contributions from in-situ ^{176}Lu decay.

In detail, Hf ratios are calculated based on measurements of radiogenic ^{176}Hf to its stable counterpart, ^{177}Hf. We report the measured $^{176}Hf/^{177}Hf$ in epsilon units (ε), which track changes of the $^{176/177}Hf$ ratio in the 4th decimal place, normalized to the $^{176}Hf/^{177}Hf$ ratio of the Chondritic Uniform Reservoir (CHUR). Epsilon Hf is calculated by the following equation (Equation 1):

$$\varepsilon Hf_t = \left\{ \left[\left(^{176}Hf/^{177}Hf\right)^{t}_{sample} / \left(^{176}Hf/^{177}Hf\right)^{t}_{CHUR} \right] - 1 \right\} \times 10^4 \quad (1)$$

where εHf is equal to normalizing the $^{176}Hf/^{177}Hf$ ratio of an unknown to the Chondritic Uniform Reservoir (CHUR) at a given time and multiplying the quotient by 10,000 (Equation 1). For details regarding instrumentation, interference and fractionation corrections, measurement methods, and sample standard bracketing techniques, please refer to the Supporting Information S1.

We present our Hf and zircon U-Pb data in combined plots from 120 to 40 Ma using plotter software provided by Vermeesch et al. (2016) and Sundell et al. (2019). Individual sample plots from oldest to youngest can be found in the Supporting Information S2. In order to evaluate the Hf data, we calculated the standard error using 4 Myr bins (Figures 4 and 5). We interpret εHf_t trends toward lower, evolved values to represent partial melting of crustal affinity domains and trends toward higher, juvenile values to reflect partial melting of mantle affinity domains (see also Bahlburg et al., 2009, 2010). εHf_t shifts can be driven by compositional changes in the upper or lower plate. All biostratigraphic ages were taken from Wolfgring et al. (2017) and Ocakoğlu et al. (2018) and compared to detrital zircon maximum depositional ages from samples published by Mueller et al. (2019, 2022). To remain as objective as possible, we used a stochastic approach to calculating zircon maximum depositional ages based on a software provided by Keller et al. (2018). Zircon Kernel Density Estimates (KDE's) were calculated for U-Pb ages from 120 to 40 Ma using 1.5 Myr bins unless stated otherwise. We refer the reader to Figure 2 for general sample locations and Figure 3 for the justification of the sample order reported in Table 1, which also contains GPS coordinates, biostratigraphic and zircon maximum depositional ages. See Supporting

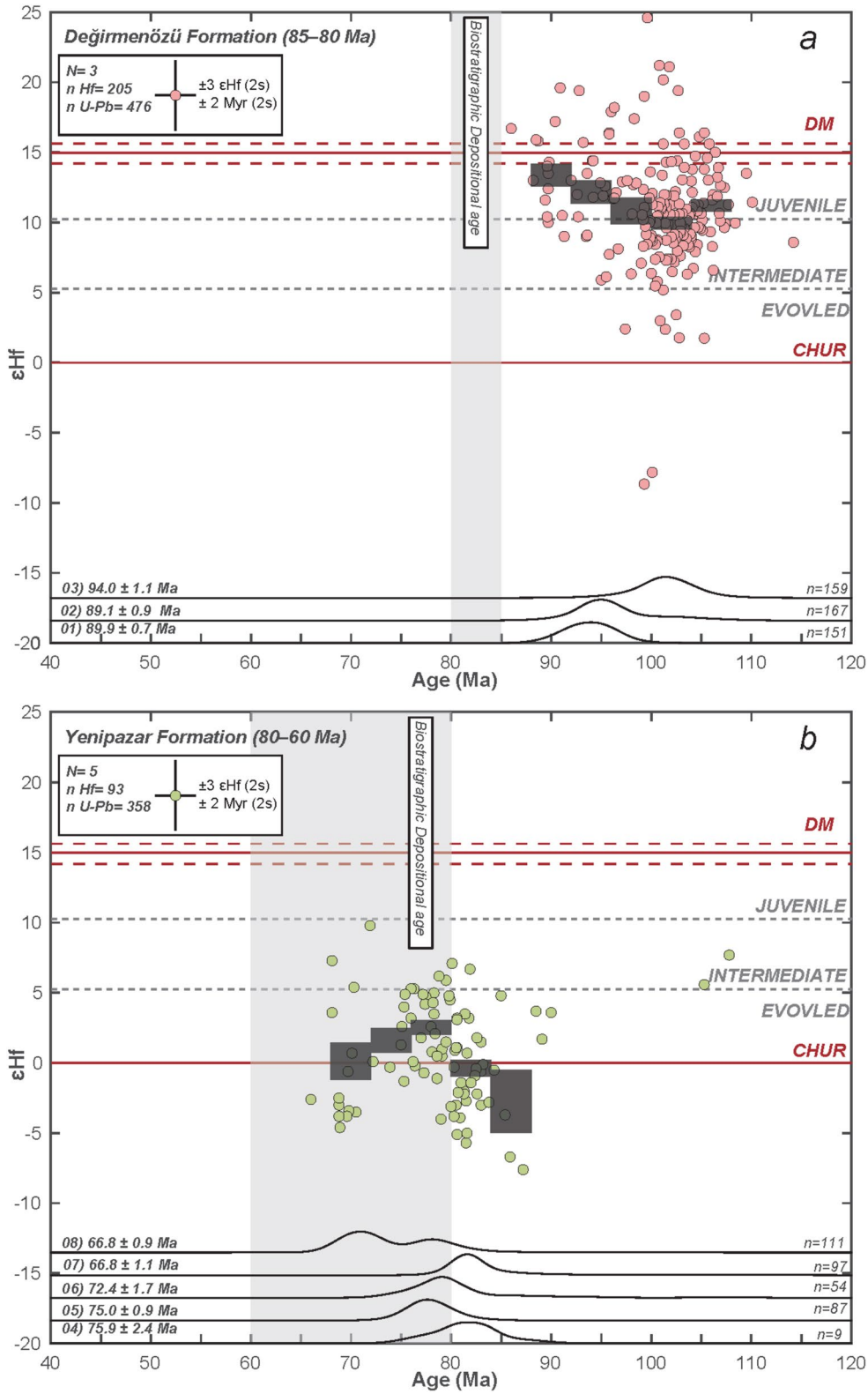

Figure 4. Zircon U-Pb versus εHf data from (a) the stratigraphically lower 85–80 Ma Değirmenözü Formation and (b) the overlying 80–60 Ma Yenipazar Formation. Zircon maximum depositional ages are next to sample numbers. Gray columns reflect the units depositional age based on biostratigraphy. All "*n*" and "*n* U-Pb" reflect ages between 120 and 40 Ma. Opaque boxes display the 4 Myr binned standard error. CHUR (chondritic uniform reservoir), DM (depleted mantle).

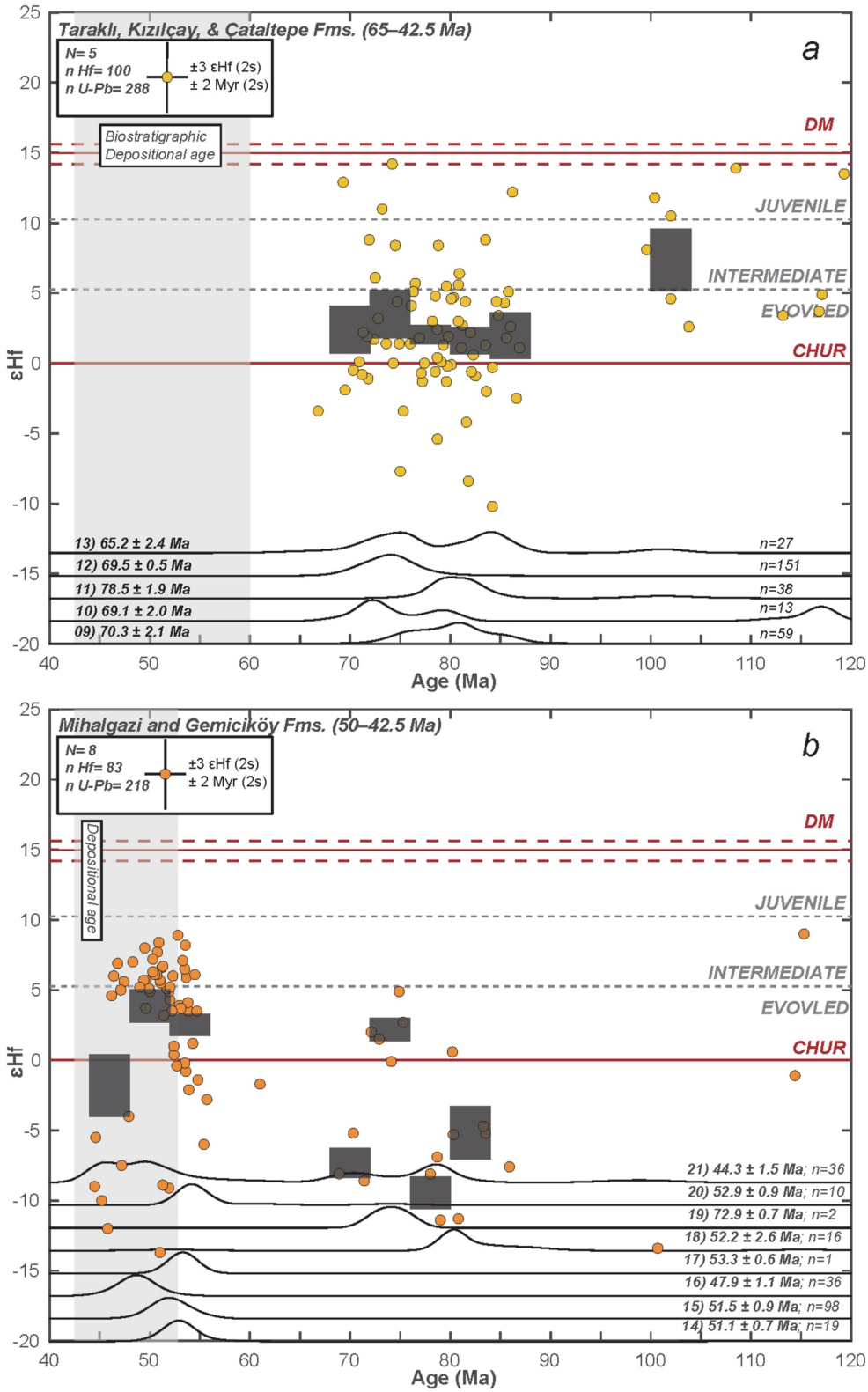

Figure 5. Zircon U-Pb versus εHf data from (a) the 65–42.5 Ma Taraklı, Kızılçay, and Çataltepe Formations which overlie the Yenipazar Formation and (b) the stratigraphically highest 50–42.5 Ma Mihalgazi and Gemiciköy Formations. Zircon maximum depositional ages are next to sample numbers. Gray columns reflect the units depositional age based on biostratigraphy. All "*n*" and "*n* U-Pb" reflect ages between 120 and 40 Ma. Opaque boxes display the 4 Myr binned standard error. CHUR (chondritic uniform reservoir), DM (depleted mantle).

Table 1
Sample Details

Sample	Formation/ Section	Epoch: Age	Marker	(Biostratigraphic) age (Ma)	Zircon U-Pb MDA (Ma) ± 2 s	Latitude (DD)	Longitude (DD)
21. 17MGB02	Gemicikoy/YS	Eocene: Lutetian–Bartonian?	*Morozovelloides Lehneri*	42.3–42.5	43.3 ± 1.5[a]	40.21044	30.61553
20. 16SKY50	Mihalgazi/SCS	Eocene: Ypresian–Lutetian?	–	–	52.9 ± 0.9	40.07864	30.74472
19. 16SKY42	Mihalgazi/SCS	Eocene: Ypresian–Lutetian?	–	–	72.9 ± 0.7	40.07450	30.74394
18. 15YP09	Mihalgazi/SCS	Eocene: Ypresian–Lutetian?	–	–	52.2 ± 2.6	40.06944	30.74389
17. 16SKY26	Mihalgazi/SCS	Eocene: Ypresian–Lutetian?	–	–	53.3 ± 0.6	40.05858	30.68808
16. 15YP07	Mihalgazi/SCS	Eocene: Ypresian	Tuff	–	47.9 ± 1.1[b]	40.05222	30.62028
15. 15YP11	Mihalgazi/SCS	Eocene: Ypresian	Tuff	–	51.5 ± 0.9[b]	40.05222	30.62028
14. 16SKY04	Mihalgazi/SCS	Eocene: Ypresian	–	–	51.1 ± 0.7	40.03025	30.65231
13. 18TK01	Cataltepe/TS	Eocene: Ypresian	*Morozovelloides Lehneri*	54.7–55.9	65.2 ± 2.4	40.32783	31.52086
12. 18KIZ01	Kizilcay/OS	Eocene: Ypresian	*Morozovelloides Lehneri*	<55.9	69.5 ± 0.5	40.39667	30.96286
11. 15YP14	Kizilcay/YS	Eocene: Ypresian	*Morozovelloides Lehneri*	66.0–59.2	78.5 ± 1.9	40.16722	30.52194
10. 18TBTG	Tarakli/TS	Paleocene: Danian–Selandian	*Morozovella angulata*	59.2–55.9	69.1 ± 2.0	40.35511	31.52228
09. 18TB01	Tarakli/TS	Paleocene: Danian–Selandian	*Morozovella angulata*	61.0–59.2	70.3 ± 2.1	40.35756	31.52444
08. 15YP13	Yenipazar/YS	Paleocene: Danian	Tuff	–	66.8 ± 1.1[b]	40.16722	30.52194
07. 18NAL12	Yenipazar/NS	Paleocene: Danian	K-Pg boundary	66.0–61.2	66.8 ± 0.9[a]	40.24503	31.30947
06. 15G002	Yenipazar/GS	Late Cretaceous: Campanian	*Globotruncana ventricosa*	75.7–79.5	72.4 ± 1.7[a]	40.40583	30.78611
05. 15G001	Yenipazar/GS	Late Cretaceous: Campanian	Tuff	–	75.0 ± 0.9[b]	40.39611	30.78083
04. 18NAL05	Yenipazar/NS	Late Cretaceous: Campanian	Biomarker CC21	77.6–76.8	75.9 ± 2.4[a]	40.23506	31.30644
03.CC082918-01	Yenipazar/NS	Late Cretaceous: Campanian	*Globotruncana elevata*	79.5–83.6	94.0 ± 1.1	40.23111	31.29783
02. 18DMN01	Degirmenozu/OS	Late Cretaceous: Santonian	*Dicarinella asymeetrica*	83.6–84.8	89.1 ± 0.9	40.37392	30.97778
01. 17MGB01	Degirmenozu/GS	Late Cretaceous: Santonian	*Dicarinella asymetrica*	83.6–84.8	89.9 ± 0.7	40.44772	30.74569

Note. See Supporting Information S1 for more details. Göynük Section (GS), Nallıhan Section (NS), Okçular Section (OS), Sarıcakaya Composite Section (SCS), Taraklı Section (TS), Yenipazar Section (YS).
[a]U-Pb MDA = Biostrat age. [b]tuff—no data.

Information S1 for a comparison of maximum depositional age metrics, raw Hf data, CL images, and reduced data for reproducing the plots described in the following section.

5. Results

Below we describe our zircon U-Pb and Hf results from 120 to 40 Ma (Figures 4 and 5). Based on our simplified stratigraphic correlation (Figure 3) we describe samples from oldest to youngest. For simplicity, all stratigraphic thicknesses are taken from the Yenipazar Section. Section 5.3 provides a condensed summary of the results further illustrated in Figure 6.

5.1. The Upper Cretaceous Section of the Central Sakarya Basin

We collected three zircon U-Pb samples from Değirmenözü Formation (01–03; Table 1), located within the basal ∼100 m of Central Sakarya basin (Figure 3). Based on the presence of *Dicerinella asymetrica* and *Globotruncanita elevata*, biostratigraphic correlation indicates the Değirmenözü Formation was deposited from ca. 85–80 Ma. In contrast, zircon U-Pb maximum depositional ages range from ca. 95–90 Ma (Table 1) and are associated with age peaks from 105 to 90 Ma. Mean εHf values plot in the juvenile realm at ≥10 ε units and increase to ∼14 ε units between 105 and 90 Ma (Figure 4a).

The Yenipazar Formation consists of five zircon U-Pb samples (04–08; Table 1) and represents the remainder of the upper Cretaceous section, from the equivalent of 100–1,000 m in the Yenipazar section (Figure 3). Based

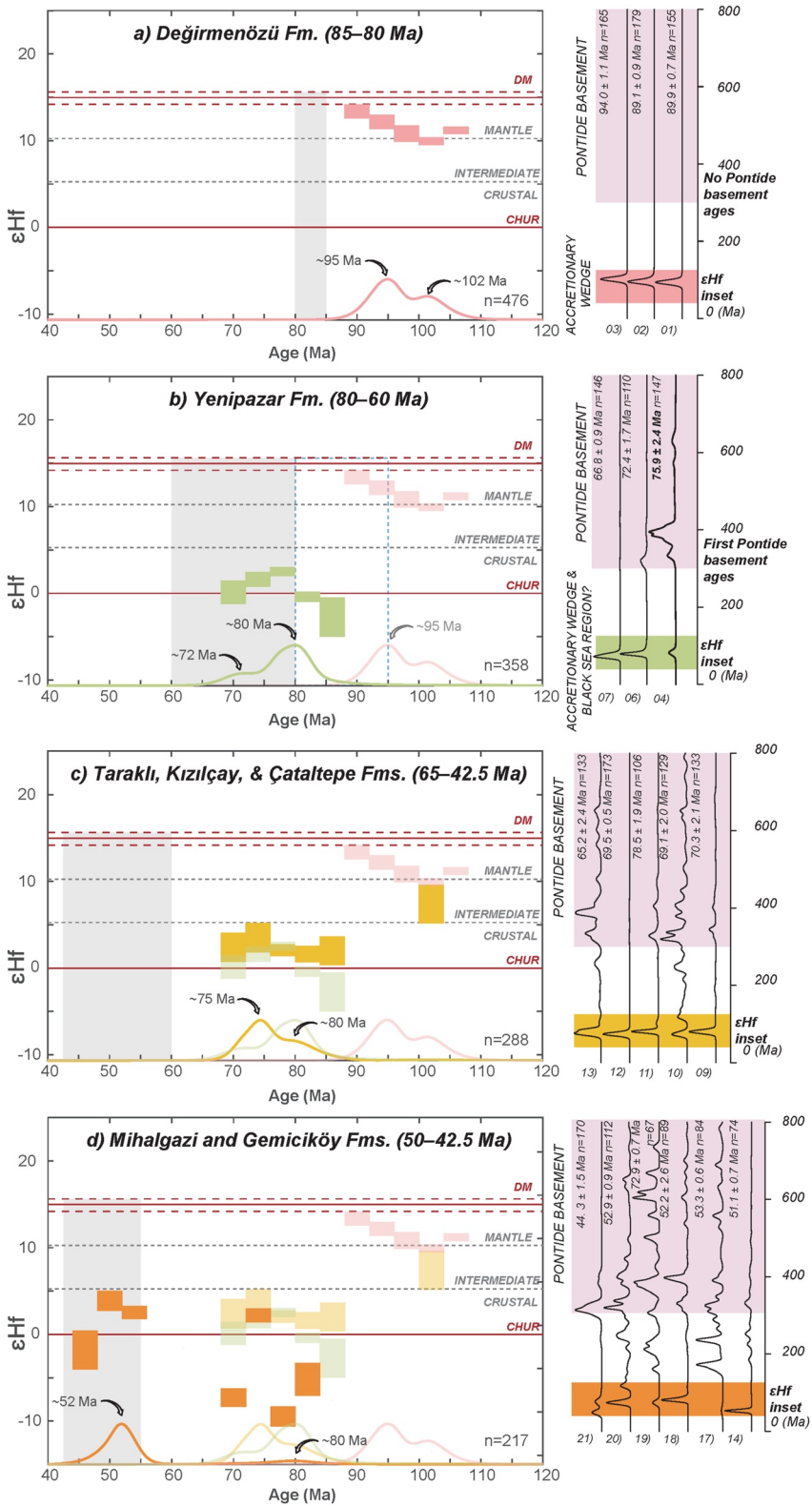

Figure 6.

on stratigraphic correlations by Ocakoğlu et al. (2018), which takes into account the presence of *Globotruncanita ventricosa*, the K-Pg boundary, and the U-Pb depositional age of an ash fall tuff (08; 66.8 ± 1.1 Ma; Table 1) immediately below the contact with Kızılçay Formation, the Yenipazar Formation was deposited from ca. 80–60 Ma. Zircon U-Pb maximum depositional ages range from 80 to 65 Ma (Table 1) and are associated with zircon U-Pb age peaks from 90 to 65 Ma. Mean εHf values plot in the evolved realm (ca. −2.5 ε units) and are initially ∼12 ε units lower than those from the Değirmenözü Formation. After the transition from the juvenile to evolved domain between 95 and 80 Ma, εHf values remain in the evolved realm but increase from 80 to 75 Ma (0–2.5 ε units). From 75 to 65 Ma εHf values decrease from 2.5 to 0 εHf units (Figure 4b).

5.2. The Lower–Middle Paleogene Section of the Central Sakarya Basin

The Taraklı (09–10; Table 1), Kızılçay (11–12; Table 1), and Çataltepe formations (13; Table 1) are characterized by 5 zircon U-Pb samples collected from the equivalent of 1,000–2,200 m into the Yenipazar section (Figure 3). Based on the presence of *Racemiguembelina fructicosa* and *Morozovella angulata* within the Taraklı and Kızılçay Formations and *Morozovelloides lehneri* in the overlying Güvenç Formation, stratigraphic correlation indicates these formations were deposited from ca. 65–42.5 Ma (Ocakoğlu et al., 2018). Zircon U-Pb maximum depositional ages range from ca. 77.5–70.0 Ma (Table 1) and are associated with age peaks from 90 to 65 Ma. Mean εHf values are generally constant and plot at ∼2.5 εHf units within the evolved domain. A secondary age-peak from 110 to 105 Ma yields intermediate εHf values (Figure 5a).

The Mihalgazi (14–20; Table 1) and Gemiciköy Formations (21; Table 1) are characterized by eight samples and reflect deposition within the Sarıcakaya basin and the highest stratigraphic levels of the Central Sakarya basin (Figure 3). Based on the presence of two ash fall tuffs (15; 51.5 ± 0.9 Ma and 16; 47.9 ± 1.1 Ma; Table 1) in the basal ∼200 m of the section, the Mihalgazi Formation was deposited after ∼50 Ma. In turn, the Gemiciköy Formation was deposited after ∼42.5 Ma, based on the presence of *Morozovelloides lehneri* within the underlying Güvenç Formation. Zircon U-Pb depositional ages above the two tuffs generally cluster between 53 and 44 Ma. Zircon age peaks are variable and occur from 85 to 65 Ma and 60–45 Ma. From 90 to 65 Ma mean εHf values plot in the evolved realm (−10–2.5 ε units) with no clear trend. From 60 to 50 Ma mean εHf values plot in the evolved realm (∼2.5 ε units) and decrease significantly by ∼45 Ma (Figure 5b).

5.3. Results Summary

The Değirmenözü Formation (01–03; Table 1) was deposited from ca. 85–80 Ma. However, zircon maximum depositional ages are 5–10 Myr older than biostratigraphic depositional ages and range from ca. 95–90 Ma. Significant zircon age peaks occur at 102 and 95 Ma associated with juvenile mean εHf values. No Devonian–Carboniferous detrital zircon U-Pb ages occur within the Değirmenözü Formation (Figure 6a).

The Yenipazar Formation (04–08; Table 1) was deposited from ca. 80–60 Ma. Zircon maximum depositional ages generally overlap with biostratigraphic depositional ages and range from ca. 80–65 Ma. Significant zircon age peaks occur at 80 and 72 Ma, associated with evolved mean εHf values. Two of the three detrital zircon samples exhibit Devonian–Carboniferous U-Pb ages (Figure 6b).

The Kızılçay, Taraklı, and Çataltepe formations (09–13; Table 1) were deposited from ca. 65–42.5 Ma. However, ca. 75–65 Ma zircon maximum depositional ages are generally older than biostratigraphic depositional ages. Significant zircon age peaks occur at 80 and 75 Ma associated with evolved mean εHf values. Four of the five detrital zircon samples exhibit Devonian–Carboniferous U-Pb ages (Figure 6c).

The Mihalgazi and Gemiciköy formations (14–21; Table 1) were deposited around ca. 50–42.5 Ma. Zircon maximum depositional ages generally overlap or are slightly older than biostratigraphic depositional ages and range from ca. 53–44 Ma. A significant zircon age peak associated with evolved mean εHf values occurs at 80 Ma.

Figure 6. Simplified U-Pb versus mean εHf plots. Gray column reflects the given formations depositional age. Tuffs omitted from DZ plots (05, 08, 15, 16). For comparison, data from the underlying plots are superimposed semi-opaquely. Panel (a) the 85–80 Ma Değirmenözü Formation exhibits juvenile mean εHf values with age peaks at 102 and 95 Ma. Panel (b) the 80–60 Ma Yenipazar Formation exhibits evolved εHf values with age peaks at 80 and 72 Ma and the first appearance of Devonian–Carboniferous basement zircon ages. Panel (c) the 65–42.5 Ma Taraklı, Kızılçay and Çataltepe formations exhibit mean εHf values with age peaks at 80 and 75 Ma that overlap with the underlying Yenipazar Formation. Panel (d) the 50–42.5 Ma Mihalgazi and Gemiciköy Formations exhibit mean εHf values with age peaks at 80 and 52 Ma that overlap with, but are also more evolved than the underlying formations.

Mean εHf values at 52 Ma are associated with less evolved values. All of the detrital zircon samples exhibit Devonian–Carboniferous U-Pb ages (Figure 6d).

6. Single Versus Double Subduction Models

We limit our schematic reconstruction to a 2-D transect that passes through the Central Sakarya basin and generalized paleogeographic maps based on van Hinsbergen et al. (2016). Our main goal is to determine if one or two subduction zones accommodated convergence, not the precise kinematic evolution of the region. We refer the reader to Kaymakçı et al. (2009), van Hinsbergen et al. (2016, 2020) and Gürer et al. (2016) for more detailed paleogeographic reconstructions.

Kinematic results from van Hinsbergen et al. (2016) indicate ∼1,000 km of convergence was accommodated between the Anatolide-Tauride Block and the Pontides from 100 to 60 Ma. Thus, prior to the ∼750 km of upper plate extension within the İzmir-Ankara Ocean (van Hinsbergen et al., 2016, 2020) from ca. 105–95 Ma, the Anatolide-Tauride Block and the Pontides were likely separated by a ∼250 km swath of oceanic lithosphere. In our schematic reconstruction we accommodate each 5 Myr timestep from 95 to 80 Ma with ∼250 km of convergence (i.e., 5 cm/a), followed by the remaining ∼250 km of convergence from 80 to 60 Ma in equal 10 Myr timesteps (i.e., 1.25 cm/a), broadly according to van Hinsbergen et al. (2016, 2020). We partition equal amounts of convergence via subduction below the Sakarya Zone and obduction above the Anatolide-Tauride Block from 95 to 90 Ma. From 90 to 70 Ma we accommodate all convergence below the Sakarya Zone. After 70 Ma, we accommodate the remaining ∼125 km of convergence along the northern margin of the Anatolide-Tauride Block, based on metamorphism of the Afyon Zone (e.g., Candan et al., 2005). We arbitrarily place ∼25 km of extension in the Black Sea backarc basin prior to the first time-step from 105 to 95 Ma, followed by an additional ∼125 km from 95 to 80 Ma.

6.1. The 85–80 Ma Değirmenözü Formation

It is difficult to determine if the juvenile 102 and 95 Ma zircon age peaks from the Değirmenözü Formation (Figure 6a) support or refute the single subduction zone model. Direct evidence for Albian plutonic rocks along the southern margin of Eurasia have yet to be identified (Okay & Nikishin, 2015). However, subsurface data, extrusive volcaniclastic horizons, and Albian age peaks within detrital zircon samples collected from late Cretaceous–Eocene sedimentary rocks from the Crimean Peninsula (Nikishin et al., 2012, 2015, 2017) support local volcanism at this time. Thus, if the juvenile 102 and 95 Ma detrital zircon age peaks within the Değirmenözü Formation were sourced from Crimea, flat slab subduction must have occurred within the Neotethys. However, to explain the juvenile 102 and 95 Ma zircon age peaks, the slab must have dipped more steeply proximal to the southern margin of Eurasia and resulted in upper plate extension. Rapid convergence rates (5 cm/a) in conjunction with incipient subduction of the more buoyant Tauride passive margin (Tavşanlı Zone) attached to previously subducted, less buoyant oceanic lithosphere could explain such a scenario.

However, Albian subduction erosion (e.g., Okay et al., 2013; Okay, Tüysüz, et al., 2006) and the significant erosional surface between Jurassic and Cretaceous levels of the Sakarya Zone (map units JLK and UKMP Figures 2 and 3; Altıner et al., 1991) support a scenario where flat slab subduction would have continued beneath the Pontides. Furthermore, flat slab subduction generally drives thick-skinned basement exhumation along the upper plate. One such example in Anatolia is the Triassic Cimmerian Orogeny, where underthrusting of Karakaya Complex (e.g., Okay et al., 2002) resulted the development of an unconformity between the Devonian–Triassic basement and Jurassic–early Cretaceous transitional marine sedimentary rocks (map units DT and JLK; Figures 2 and 3). Thus, within the single subduction model it is difficult to explain the absence of Devonian–Carboniferous detrital zircon, significant of exhumed Pontide basement and isotopically evolved late Cretaceous Hf isotopes significant of crustal thickening in the Değirmenözü Formation (Figure 6a; T. Ustaömer et al., 2016, 2020).

The single subduction zone model further necessitates that late Cretaceous detrital zircon within the Değirmenözü Formation, which was sourced from the İzmir-Ankara suture zone (Figure 3) were originally part of the Pontide forearc. The simplest way to reconcile why 95–90 Ma zircon maximum depositional ages do not reflect the 85–80 Ma biostratigraphic age of the Değirmenözü Formation is to invoke a scenario where portions of the Pontide forearc bypassed the outer arc high and were deposited within the subduction zone trench. In turn, the trench fill must have been reworked from south to north through the İzmir-Ankara accretionary prism (e.g., Noda, 2016) and deposited into the Central Sakarya basin during a coeval magmatic hiatus.

In contrast, the double subduction zone model reconciles juvenile 102 and 95 Ma zircon age peaks within the Değirmenözü Formation, which were sourced from the İzmir-Ankara suture zone (Figure 6a) in terms of crustal thinning during ~750 km of supra-subduction zone extension in the İzmir-Ankara Ocean (Figures 7a and 7b; e.g., Pearce et al., 1984; Robertson, 2004; Yalınız, 2008). We note that this model is different from Kaymakçı et al. (2009) in that we believe two north dipping subduction zones had been established by Albian times. However, in our model magmatism in Crimea, subduction erosion and exhumation in the Pontides would have instead been driven by the additional north dipping subduction zone along the southern margin of the Pontides from 105 to 90 Ma (Figures 7a and 7c). Importantly, however, by 85 Ma ~500 km of convergence was accommodated between the Pontides and Taurides. Thus, we explain the absence of Devonian and Carboniferous detrital zircon and presence of isotopically juvenile late Cretaceous Hf isotopes in conjunction with 5–10 Myr lag times from the Değirmenözü Formation (Figure 6a) as the development and subsequent reworking of an isolated supra-subduction zone retroarc basin through the accretionary prism and into the Central Sakarya basin beginning around ~85 Ma (Figure 7d).

6.2. The 80–60 Ma Yenipazar Formation

The overlying Yenipazar Formation exhibits evolved 80 and 72 Ma zircon U-Pb age peaks as well as Carboniferous and Devonian detrital zircon age populations (Figure 6b). Such observations could be explained by the single subduction zone model in terms of crustal thickening and basement exhumation as ~750 km of convergence was accommodated from 95 to 80 Ma. However, the transition from juvenile to evolved εHf values occurred rapidly between 95 and 80 Ma (Figure 6b) and is thus seemingly inconsistent with the more gradual process of crustal thickening (e.g., Sundell et al., 2022). In this vein, 80 and 72 Ma zircon U-Pb age peaks whose magnitude of crustal contamination decreases through time (Figure 6b) could reflect the combined effects of magmatic assimilation of Neoproterozoic and Paleozoic Pontide basement assemblages (Şengör et al., 1984; A. Ustaömer et al., 2005; T. Ustaömer et al., 2013) during slab rollback and southward arc migration (Ocakoğlu et al., 2018). Thus, documented uplift and subaerial exposure of the İzmir-Ankara accretionary prism in Campanian times, evidenced by increasing Ni/Zr ratios (Ocakoğlu et al., 2018) could be reconciled by topographic doming as a result of southward arc migration.

In contrast, the double subduction zone model explains the rapid transition from juvenile to evolved εHf values between 95 and 80 Ma in terms of subduction and partial melting of the Tauride passive margin within the intra-oceanic subduction zone. Importantly, the isotopic pull-down between 95 and 80 Ma is more or less identical to the timing of ophiolite obduction (van Hinsbergen et al., 2016 and references therein) and subduction of the Tauride passive margin Tavşanlı Zone within the İzmir-Ankara Ocean (Mulcahy et al., 2014; Okay & Kelley, 1994; Plunder et al., 2015; Pourteau et al., 2019; Seaton et al., 2009, 2014; Sherlock et al., 1999). Thus, based on the timing and the rapid nature of the isotopic shift (Figure 6b) the data seem more consistent with subduction and partial melting of silicious Tauride passive margin sedimentary rocks (Figure 7d). In turn, the sequential underthrusting of the intra-oceanic basin along the southern margin of the Sakarya zone would also explain uplift of the accretionary prism by ~80 Ma (Ocakoğlu et al., 2018). Finally, the decreasing magnitudes of crustal contamination from 80 to 72 Ma (Figure 6b) may reflect slab breakoff along the intra-oceanic subduction zone (Figure 7e; Okay & Whitney, 2010).

The Cenomanian–Maastrichtian Saraçköy volcanic suite (Koçyíğít et al., 2003) and the Beypazari granitoid (Öztürk et al., 2012; Speciale et al., 2012) are due east of the Central Sakarya basin. They exhibit moderately evolved isotopic signatures indicative of crustal contamination (Öztürk et al., 2012), and are structurally imbricated into the İzmir-Ankara accretionary mélange (Koçyíğít et al., 2003). Such plutonic bodies are interpreted to have been emplaced outboard of the Pontides (Koçyíğít et al., 2003). Thus, these observations are inconsistent with crustal contamination coming from the upper plate. In this light, if the Tauride passive margin subducted and was subject to partial melting outboard of the Sakarya Zone, it is difficult to explain coeval magmatism within the Pontides to the north (Görür, 1988, 1997; Görür et al., 1993; Hippolyte et al., 2010, 2018; Okay et al., 1994; Robinson, 1997; Tüysüz, 1999; Tüysüz & Tekin, 2007) without an additional subduction zone.

We emphasize that the double subduction zone model does not necessitate that all late Cretaceous detrital zircon within the Central Sakarya basin was sourced from reworked portions of the intra-oceanic basin. Instead, the double subduction zone framework describes a scenario where the Central Sakarya basin was initially sourced from the İzmir-Ankara accretionary prism beginning around 85 Ma, followed by additional input from the Sakarya Zone beginning around 75 Ma (Figure 7f), based on the first appearance of Devonian–Carboniferous

10.1029/2022GC010481

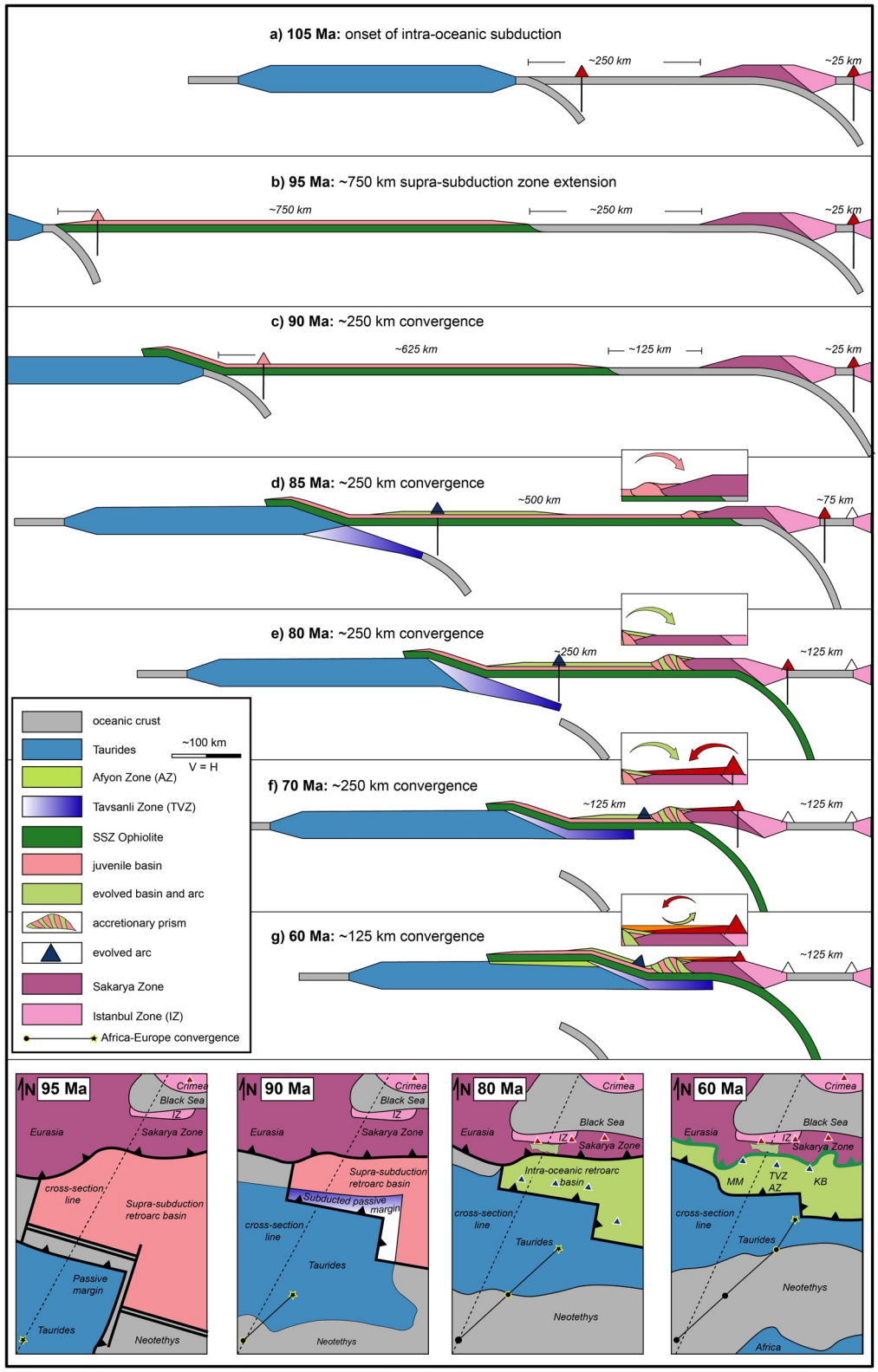

Figure 7.

detrital zircon (Figure 6b). However, if the Devonian–Carboniferous detrital zircon were instead sourced from the Anatolide-Tauride Block (T. Ustaömer et al., 2020), and the Central Sakarya basin was thus wholly sourced from the south—including late Cretaceous detrital zircon age populations—the presence of coeval magmatism within the Pontides would still be difficult to justify with only a single subduction zone.

Importantly, remnants of this intra-oceanic subduction zone system have yet to be identified directly south of the Central Sakarya basin. Furthermore, the contact between late Cretaceous levels of the Central Sakarya basin and the accretionary prism have yet to be identified. We suggest the absence of an imbricated island arc within the accretionary prism of the Western Pontides may be related to the high-angle subduction of the Tavşanlı Zone, whereas the presence of an imbricated island arc in the Central Pontides may be related to the low-angle subduction of the Kirşehır Block (e.g., van Hinsbergen et al., 2016). We also speculate that the contact between late Cretaceous levels of the Central Sakarya basin and the accretionary prism may be covered as a result of thrust faulting related to ongoing shortening in to middle–late Cenozoic times.

Alternatively, evolved detrital zircon within the Central Sakarya basin could have been sourced from the Saraçköy volcanic suite, the Beypazari granitoid (Koçyiğit et al., 2003; Öztürk et al., 2012; Speciale et al., 2012), or the Kocaeli basin within the İstanbul Zone (Figure 1 (KOC); Akbayram, Şengör, & Özcan, 2016). However, if the Central Sakarya basin underwent similar magnitudes of counterclockwise rotations (15–35°) as the Ankara region (Figure 1; Özkaptan et al., 2021) apparent paleocurrents would no longer point to sources from the southeast and east (Figure 3). In turn, the Kocaeli basin has been translated 50–80 km west during Neogene right lateral motion along the Northern Anatolian Fault (Akbayram, Sorlien, & Okay, 2016; Hubert-Ferrari et al., 2002). Thus, westward translation of the Kocaeli basin in conjunction with the paucity of paleocurrents sourced from the north (Figure 3) make the İstanbul Zone an unlikely source.

6.3. Paleogene Transitional Marine and Terrestrial Section

Closure of the ∼1,000 km wide İzmir-Ankara Ocean in Western Anatolia (van Hinsbergen et al., 2016) was followed by collision between 80 and 60 Ma (e.g., Ballato et al., 2011; Cavazza et al., 2012; Gülyüz, 2020; Gülyüz et al., 2019; Mueller et al., 2022; Okay et al., 2020). At this juncture in the region's geodynamic evolution, both the single and double subduction zone models are more or less identical. Evolved 80 and 75 Ma age peaks within the Paleogene Taraklı, Kızılçay, and Çataltepe Formations overlap with those of the underlying Yenipazar Formation (Figure 6c), and thus likely reflect intra-basinal unroofing (Figure 7g). This interpretation is supported by local unconformities within the upper levels of the Central Sakarya basin (Ocakoğlu et al., 2018), detrital zircon provenance, and sandstone petrography (Mueller et al., 2019). In turn, the 50–42.5 Ma Mihalgazi and Gemiciköy Formations exhibit zircon age peaks with the most evolved isotopic signature, centered around 80 and 52 Ma (Figure 6d). Although their source remains to be determined, zircon U-Pb ages that center around 80 Ma are substantially more evolved than identically aged zircon deposited in the lower levels of the Central Sakarya basin (Figure 6d). Such observations strongly support the presence of an additional late Cretaceous volcanic center and thus two subduction zones.

Notably, the absence of isotopically distinct 102 and 95 Ma zircon U-Pb age peaks in the upper levels of the Central Sakarya basin (Figure 6d) is inconsistent with the nucleation of an additional subduction zone in Albian times (i.e., Kaymakçı et al., 2009). However, if supra-subduction zone extension was ongoing in Albian times (van Hinsbergen et al., 2016, 2020), it is difficult to explain the source of volcanism in Crimea (Nikishin et al., 2012, 2015, 2017) without an additional subduction zone. Finally, evolved 50–45 Ma zircon within the Mihalgazi and Gemiciköy formations were deposited during a period of syn-collisional magmatism along the İzmir-Ankara (e.g., Harris et al., 1994) and Intra-Pontide (Kasapoğlu et al., 2016) suture zones, whose geodynamic significance remain debated (see Mueller et al., 2019 and references therein).

Figure 7. Preferred double subduction zone model. Crustal scale cross section synthesizing the datasets discussed in this manuscript from 105 to 60 Ma. Plan view paleogeography is generalized and correspond to cross-sections b, c, e, and g along the dotted line. Insets in (d–g) illustrate the development of the Central Sakarya basin. (a) 105 Ma; intra-oceanic subduction zone nucleation. (b) 95 Ma; ∼750 km of supra-subduction zone extension. (c) 90 Ma; Ophiolite obduction above the intra-oceanic subduction zone. (d) 85 Ma; subduction of the Tauride passive margin resulting in formation of the Tavşanlı Zone and structural imbrication and redeposition of the juvenile intra-oceanic basin into the Central Sakarya basin. (e) 80 Ma; underthrusting of evolved portions of the intra-oceanic basin, exhumation and redeposition of the evolved intra-oceanic basin into the Central Sakarya basin. (f) 70 Ma; intra-oceanic arc collision, exhumation and redeposition of the evolved intra-oceanic basin into the Central Sakarya Basin. (g) 60 Ma; onset of intercontinental collision and intra-basinal unroofing within the Central Sakarya basin. SSZ, supra-subduction zone. See discussion section for details.

6.4. Geodynamic Implications of the Double Subduction Zone System in Western Anatolia

Given that the Cimmerian Orogeny marks the closure of the Paleotethys in late Triassic times (Okay et al., 2002) and 750 out of the 1,000 km swath of oceanic lithosphere separating the Pontides and Taurides at ~95 Ma (van Hinsbergen et al., 2016, 2020) formed as a result of supra-subduction zone extension beginning around 105 Ma (e.g., Pourteau et al., 2019), most of the oceanic lithosphere involved in the Anatolian double subduction zone system was quite young (i.e., Δt << 100 Myr). Furthermore, it is unclear how convergence was accommodated within the double subduction zone system. Thus, we focus the remaining discussion on how changing the length of a young middle (Anadolu) plate (e.g., Mishin et al., 2008) and subducting the Tauride passive margin (Čížková & Bina, 2015; Jagoutz et al., 2015) could have influenced the geodynamic evolution of Western Anatolia.

Numerical 2–D modeling demonstrates that the outboard subduction zone will accommodate most of the convergence given a short middle plate (500–900 km), whereas convergence will be more or less equally partitioned between both subduction zones if the middle plate is long (1,100–1,300 km) (Mishin et al., 2008). Thus, the geodynamic evolution of Western Anatolia can in part be explained by changes in the length of the Anadolu plate. In this light, prior to ~95 Ma, the region's geodynamic evolution can be described in terms of a short plate (i.e., <900 km), dominated by the outboard intra-oceanic subduction zone. Importantly this could explain the absence of a well-developed magmatic arc throughout Crimea in Albian times (e.g., Okay & Nikishin, 2015), which was instead dominated by widespread supra-subduction zone extension within the Neotethys (e.g., Göncüoğlu et al., 2006, 2010; Manav et al., 2004; Önen, 2003; Sarıfakıoğlu et al., 2009, 2010, 2017; van Hinsbergen et al., 2016). In turn, from 95 Ma onward the region's geodynamic evolution can be described in terms of a long middle plate (~1,000 km), where the total convergence would have been partitioned between the two north dipping subduction zones. Such a scenario could explain the resumption of volcanism along the southern margin of Eurasia (Nikishin et al., 2015).

Furthermore, similar to the double subduction zone model used to describe the Philippine region (Faccenna et al., 2018; Holt et al., 2018; Čížková & Bina, 2015), upon the partial subduction of the Tauride passive margin at ~85 Ma, the middle plate may have buckled within the double subduction zone system. In turn, buckling of the Anadolu plate could have decreased overall convergence rates and resulted in the rapid sinking and breakoff (Okay & Whitney, 2010) of previously subducted oceanic crust within the intra-oceanic subduction zone. In turn, the reduction in overall convergence rates may have also driven hinge retreat along the southern margin of Eurasian margin and served as the impetus for rift-to-drift tectonism in the Black Sea backarc basin (e.g., Čížková & Bina, 2015; Görür, 1988; Görür et al., 1993; Holt et al., 2017, 2018; Mishin et al., 2008; Okay et al., 1994; Pusok & Stegman, 2019; Tüysüz, 1999).

7. Conclusions

We tested single and double subduction zone models describing the geodynamic evolution of Western Anatolia by identifying the remnants of an intra-oceanic arc within the Central Sakarya basin. The basal levels of the Central Sakarya basin are sourced from the local accretionary prism and exhibit a demonstrative shift from juvenile to evolved εHf values between 95 and 80 Ma. This isotopic excursion is best explained as recording subduction and partial melting of the Tauride passive margin Tavşanlı Zone outboard of the Eurasian margin. Thus, coeval magmatism further north within Eurasia was likely connected to an additional subduction zone. In this light, the northward translation of the Anatolide-Tauride Block was accommodated by north dipping subduction zones located along the southern margin of Eurasia and within the Neotethys. Broadly speaking, geodynamic models describing the evolution of same-dip double subduction zone systems based on changes in the length and buckling of a middle plate explain late Cretaceous supra-subduction zone extension within the Neotethys and the transition from rifting to drifting in the Western Black Sea backarc basin.

Data Availability Statement

All Hf data collected in this paper can be accessed through "earthchem.org; Campbell et al. (2023) (https://ecl.earthchem.org/view.php?id=2742)." Plotter software can be found in Vermeesch et al. (2016) (https://doi.org/10.1016/j.sedgeo.2016.01.009) and Sundell et al. (2019) (https://doi.org/10.1016/B978-0-12-816009-1.00014-9). Maximum depositional age software from Keller et al. (2018) (https://doi.org/10.7185/geochemlet.1826).

MATLAB data analysis tool can be found in the supplemental materials (https://github.com/ClayFC/binned-mean.git).

Acknowledgments
This research is supported by the U.S. National Science Foundation grant NSF EAR 1543684 to K.C.B. and M.H.T. We extend a warm thanks to B. Kurtoğlu, S. Mattingly, C. Ocakoğlu, and M. Wood for field assistance during various stages of this project. We also recognize J. Oalmann, and T. Tenpenny at The University of Kansas Isotope Geochemistry Laboratory and M. Pecha, K. Sundell, and N. Giesler at the Arizona LaserChron Center for analytical assistance. K. Sundell and N. McLean provided assistance regarding the statistical treatment of Hf datasets. We appreciate the careful handling of this manuscript by P. van der Beek and thorough reviews from N. Kaymakçı, E. Gülyüz, and an anonymous reviewer. D.J.J. van Hinsbergen, G. Topuz, and E. Cowgill significantly improved an earlier version of the manuscript.

References

Aitchison, J. C., Davis, A. M., Liu, J., Luo, H., Malpas, J. G., McDermid, I. R., et al. (2000). Remnants of a Cretaceous intra-oceanic subduction system within the Yarlung–Zangbo suture (southern Tibet). *Earth and Planetary Science Letters*, *183*(1–2), 231–244. https://doi.org/10.1016/S0012-821X(00)00287-9

Akbaş, B., Akdeniz, N., Aksay, A., Altun, E., Balci, V., Bilginer, E., et al. (2011). *Geologic map of Turkey (Scale 1:1,250,000)*. General Directorate of Mineral Exploration and Research (MTA).

Akbayram, K., Şengör, A. C., & Özcan, E. (2016). The evolution of the intra-Pontide suture: Implications of the discovery of late Cretaceous–early Tertiary melanges. *Geological Society of America Special Papers*, *525*, SPE525-18. https://doi.org/10.1130/2016.2525(18)

Akbayram, K., Sorlien, C. C., & Okay, A. I. (2016). Evidence for a minimum 52±1 km of total offset along the northern branch of the North Anatolian Fault in northwest Turkey. *Tectonophysics*, *668*, 35–41. https://doi.org/10.1016/j.tecto.2015.11.026

Aksay, A., Pehlivan, Ş., Gedik, İ., Bılginer, E., Duru, M., Akbaş, B., & Altun, I. (2002). *Geologic map of Turkey (Zonguldak, Scale 1:500,000)*. General Directorate of Mineral Exploration and Research (MTA).

Altıner, D., Koçyiğit, A., Farinacci, A., Nicosia, U., & Conti, M. A. (1991). Jurassic, Lower Cretaceous stratigraphy and paleogeographic evolution of the southern part of north-western Anatolia. *Geologica Romana*, *28*, 13–80.

Bahlburg, H., Vervoort, J. D., & DuFrane, S. A. (2010). Plate tectonic significance of Middle Cambrian and Ordovician siliciclastic rocks of the Bavarian facies, Armorican terrane assemblage, Germany—U-Pb and Hf isotope evidence from detrital zircons. *Gondwana Research*, *17*(2–3), 223–235. https://doi.org/10.1016/j.gr.2009.11.007

Bahlburg, H., Vervoort, J. D., Du Frane, S. A., Bock, B., Augustsson, C., & Reimann, C. (2009). Timing of crust formation and recycling in accretionary orogens: Insights learned from the western margin of South America. *Earth-Science Reviews*, *97*(1–4), 215–241. https://doi.org/10.1016/j.earscirev.2009.10.006

Ballato, P., Uba, C. E., Landgraf, A., Strecker, M. R., Sudo, M., Stockli, D. F., et al. (2011). Arabia-Eurasia continental collision: Insights from late Tertiary foreland-basin evolution in the Alborz Mountains, northern Iran. *Bulletin*, *123*(1–2), 106–131. https://doi.org/10.1130/B30091.1

Bouilhol, P., Jagoutz, O., Hanchar, J. M., & Dudas, F. O. (2013). Dating the India–Eurasia collision through arc magmatic records. *Earth and Planetary Science Letters*, *366*, 163–175. https://doi.org/10.1016/j.epsl.2013.01.023

Campbell, C. F., Mueller, M. A., Taylor, M. H., Ocakoglu, F., Möller, A., Métais, G., et al. (2023). *Zircon Hf isotopic data from the Central Sakarya Basin, NW Turkey, Version 1.0*. Interdisciplinary Earth Data Alliance (IEDA). https://doi.org/10.26022/IEDA/112742

Candan, O., Çetinkaplan, M., Oberhänsli, R., Rimmelé, G., & Akal, C. (2005). Alpine high-P/low-T metamorphism of the Afyon Zone and implications for the metamorphic evolution of Western Anatolia, Turkey. *Lithos*, *84*(1–2), 102–124. https://doi.org/10.1016/j.lithos.2005.02.005

Cavazza, W., Federici, I., Okay, A. I., & Zattin, M. (2012). Apatite fission-track thermochronology of the Western Pontides (NW Turkey). *Geological Magazine*, *149*(1), 133–140. https://doi.org/10.1080/09853111.2020.1809824

Čížková, H., & Bina, C. R. (2015). Geodynamics of trench advance: Insights from a Philippine-Sea-style geometry. *Earth and Planetary Science Letters*, *430*, 408–415. https://doi.org/10.1016/j.epsl.2015.07.004

Collins, A. S., & Robertson, A. H. (1997). Lycian melange, southwestern Turkey: An emplaced Late Cretaceous accretionary complex. *Geology*, *25*(3), 255–258. https://doi.org/10.1130/0091-7613(1997)025<0255:lmstae>2.3.co;2

Collins, A. S., & Robertson, A. H. (1998). Processes of Late Cretaceous to Late Miocene episodic thrust-sheet translation in the Lycian Taurides, SW Turkey. *Journal of the Geological Society*, *155*(5), 759–772. https://doi.org/10.1144/gsjgs.155.5.0759

Cowgill, E., Forte, A. M., Niemi, N., Avdeev, B., Tye, A., Trexler, C., et al. (2016). Relict basin closure and crustal shortening budgets during continental collision: An example from Caucasus sediment provenance. *Tectonics*, *35*(12), 2918–2947. https://doi.org/10.1002/2016TC004295

Darin, M. H., Umhoefer, P. J., & Thomson, S. N. (2018). Rapid late Eocene exhumation of the Sivas Basin (Central Anatolia) driven by initial Arabia-Eurasia collision. *Tectonics*, *37*(10), 3805–3833. https://doi.org/10.1029/2017TC004954

Demirkol, C. (1977). Üzümlü-Tuzaklı (Bilecik) dolayının jeolojisi. *Turkiye Jeoloji Kurumu Bulteni*, *20*, 9716. [in Turkish with English abstract].

Dilek, Y., Thy, P., Hacker, B., & Grundvig, S. (1999). Structure and petrology of Tauride ophiolites and mafic dike intrusions (Turkey): Implications for the Neotethyan ocean. *Geological Society of America Bulletin*, *111*(8), 1192–1216. https://doi.org/10.1130/0016-7606(1999)111<1192:SAPOTO>2.3.CO;2

Faccenna, C., Holt, A. F., Becker, T. W., Lallemand, S., & Royden, L. H. (2018). Dynamics of the Ryukyu/Izu-Bonin-Marianas double subduction system. *Tectonophysics*, *746*, 229–238. https://doi.org/10.1016/j.tecto.2017.08.011

Gehrels, G., & Pecha, M. (2014). Detrital zircon U-Pb geochronology and Hf isotope geochemistry of Paleozoic and Triassic passive margin strata of western North America. *Geosphere*, *10*(1), 49–65. https://doi.org/10.1130/GES00889.1

Gnos, E., Immenhauser, A., & Peters, T. J. (1997). Late Cretaceous/early Tertiary convergence between the Indian and Arabian plates recorded in ophiolites and related sediments. *Tectonophysics*, *271*(1–2), 1–19. https://doi.org/10.1016/s0040-1951(96)00249-1

Göncüoğlu, M. C., Marroni, M., Pandolfi, L., Ellero, A., Ottria, G., Catanzariti, R., et al. (2014). The Arkot Dağ Mélange in Araç area, central Turkey: Evidence of its origin within the geodynamic evolution of the Intra-Pontide suture zone. *Journal of Asian Earth Sciences*, *85*, 117–139. https://doi.org/10.1016/j.jseaes.2014.01.013

Göncüoğlu, M. C., Sayit, K., & Tekin, U. K. (2010). Oceanization of the northern Neotethys: Geo-chemical evidence from ophiolitic melange basalts within the İzmir–Ankara suture belt, NW Turkey. *Lithos*, *116*(1–2), 175–187. https://doi.org/10.1016/j.lithos.2010.01.007

Göncüoğlu, M. C., Turhan, N., Şentürk, K., Özcan, A., Uysal, Ş., & Yaliniz, M. K. (2000). A geotraverse across northwestern Turkey: Tectonic units of the Central Sakarya region and their tectonic evolution. *Geological Society, London, Special Publications*, *173*(1), 139–161. https://doi.org/10.1144/GSL.SP.2000.173.01.06

Göncüoğlu, M. C., Yalınız, M. K., & Tekin, U. K. (2006). Geochemistry, tectono-magmatic discrimination and radiolarian ages of basic extrusives within the Izmir–Ankara suture belt (NW Turkey): Time constraints for the Neotethyan evolution. *Ofioliti*, *31*, 25–38.

Görür, N. (1988). Timing of opening of the Black Sea basin. *Tectonophysics*, *147*(3–4), 247–262. https://doi.org/10.1016/0040-1951(88)90189-8

Görür, N. (1997). *Cretaceous syn-to postrift sedimentation on the southern continental margin of the western Black Sea Basin* (pp. 227–240). Memoirs-American Association of Petroleum Geologists.

Görür, N., Tuysuz, O., Aykol, A., Sakinc, M., Yigitbas, E., & Akkok, R. (1993). Cretaceous red pelagic carbonates of northern Turkey-their place in the opening history of the Black-Sea.

Gülyüz, E. (2020). Apatite fission track dating of the Beypazarı Granitoid: Insight for the inception of collision along the Northern Neotethys, Turkey. *Geodinamica Acta*, *32*(1), 1–10. https://doi.org/10.1080/09853111.2020.1809824

Gülyüz, E., Özkaptan, M., Kaymakci, N., Persano, C., & Stuart, F. M. (2019). Kinematic and thermal evolution of the Haymana Basin, a fore-arc to foreland basin in Central Anatolia (Turkey). *Tectonophysics*, *766*, 326–339. https://doi.org/10.1016/j.tecto.2019.06.020

Gürer, D., van Hinsbergen, D. J., Matenco, L., Corfu, F., & Cascella, A. (2016). Kinematics of a former oceanic plate of the Neotethys revealed by deformation in the Ulukışla basin (Turkey). *Tectonics*, *35*(10), 2385–2416. https://doi.org/10.1002/2016TC004206

Hall, R. (2012). Late Jurassic–Cenozoic reconstructions of the Indonesian region and the Indian Ocean. *Tectonophysics*, *570*, 1–41. https://doi.org/10.1016/j.tecto.2012.04.021

Harris, N. B., Kelley, S., & Okay, A. I. (1994). Post-collision magmatism and tectonics in northwest Anatolia. *Contributions to Mineralogy and Petrology*, *117*(3), 241–252. https://doi.org/10.1007/bf00310866

Hayward, A. B. (1984). Sedimentation and basin formation related to ophiolite nappe emplacement, Miocene, SW Turkey. *Sedimentary Geology*, *40*(1–3), 105–129. https://doi.org/10.1016/0037-0738(84)90042-3

Hippolyte, J. C., Müller, C., Kaymakci, N., & Sangu, E. (2010). Dating of the Black Sea Basin: New nannoplankton ages from its inverted margin in the Central Pontides (Turkey). *Geological Society, London, Special Publications*, *340*(1), 113–136. https://doi.org/10.1144/SP340.7

Hippolyte, J. C., Murovskaya, A., Volfman, Y., Yegorova, T., Gintov, O., Kaymakci, N., & Sangu, E. (2018). Age and geodynamic evolution of the Black Sea Basin: Tectonic evidences of rifting in Crimea. *Marine and Petroleum Geology*, *93*, 298–314. https://doi.org/10.1016/j.marpetgeo.2018.03.009

Holt, A. F., Royden, L. H., & Becker, T. W. (2017). The dynamics of double slab subduction. *Geophysical Journal International*, *209*(1), 250–265. https://doi.org/10.1093/gji/ggw496

Holt, A. F., Royden, L. H., Becker, T. W., & Faccenna, C. (2018). Slab interactions in 3-D subduction settings: The Philippine Sea Plate region. *Earth and Planetary Science Letters*, *489*, 72–83. https://doi.org/10.1016/j.epsl.2018.02.024

Hubert-Ferrari, A., Armijo, R., King, G., Meyer, B., & Barka, A. (2002). Morphology, displacement, and slip rates along the North Anatolian Fault, Turkey. *Journal of Geophysical Research*, *107*(B10), ETG 9-1–ETG 9-33. https://doi.org/10.1029/2001JB000393

Jagoutz, O., Royden, L., Holt, A. F., & Becker, T. W. (2015). Anomalously fast convergence of India and Eurasia caused by double subduction. *Nature Geoscience*, *8*(6), 475–478. https://doi.org/10.1038/NGEO2418

Kapp, P., & DeCelles, P. G. (2019). Mesozoic–Cenozoic geological evolution of the Himalayan-Tibetan orogen and working tectonic hypotheses. *American Journal of Science*, *319*(3), 159–254. https://doi.org/10.2475/03.2019.01

Kasapoğlu, B., Ersoy, Y. E., Uysal, İ., Palmer, M. R., Zack, T., Koralay, E. O., & Karlsson, A. (2016). The petrology of Paleogene volcanism in the Central Sakarya, Nallıhan Region: Implications for the initiation and evolution of post-collisional, slab break-off-related magmatic activity. *Lithos*, *246*, 81–98. https://doi.org/10.1016/j.lithos.2015.12.024

Kaya, O. (1972). Outlines of the ophiolite question in the Tavsanli region (in Turkish). *Bulletin of the Geological Society of Turkey*, *15*, 26–108.

Kaya, O., Kozur, H., Sadeddin, W., & Helvaci, H. (2001). Late Norian age for a metacarbonate unit in NW Anatolia, Turkey. *Geobios*, *34*(5), 527–532. https://doi.org/10.1016/S0016-6995(01)80067-X

Kaygusuz, A., Arslan, M., Siebel, W., Sipahi, F., & Ilbeyli, N. (2012). Geochronological evidence and tectonic significance of Carboniferous magmatism in the southwest Trabzon area, eastern Pontides, Turkey. *International Geology Review*, *54*(15), 1776–1800. https://doi.org/10.1080/00206814.2012.676371

Kaymakçı, N., Özçelik, Y., White, S. H., & Van Dijk, P. M. (2009). Tectono-stratigraphy of the Çankırı Basin: Late Cretaceous to early Miocene evolution of the Neotethyan suture zone in Turkey. *Geological Society, London, Special Publications*, *311*(1), 67–106. https://doi.org/10.1144/SP311.3

Keller, C. B., Schoene, B., & Samperton, K. M. (2018). A stochastic sampling approach to zircon eruption age interpretation. *Geochemical Perspectives Letters*, *8*, 31–35. https://doi.org/10.7185/geochemlet.1826

Ketin, İ. (1966). Tectonic units of Anatolia (Asia Minor). *Bulletin of the Mineral Research and Exploration*, *66*(66).

Koçyíğít, A., Winchester, J. A., Bozkurt, E., & Holland, G. (2003). Saraçköy Volcanic Suite: Implications for the subductional phase of arc evolution in the Galatean Arc Complex, Ankara, Turkey. *Geological Journal*, *38*(1), 1–14. https://doi.org/10.1002/gj.921

Lisenbee, A. (1972). *Structural setting of the Orhaneli ultramafic massif near Bursa, North-western Turkey* ((PhD thesis)). Pennsylvania State University.

Manav, H., Gültekin, A. H., & Uz, B. (2004). Geochemical evidence for the tectonic setting of the Harmancik ophiolites, NW Turkey. *Journal of Asian Earth Sciences*, *24*, 1–9. https://doi.org/10.1016/S1367-9120(03)00018-X

McQuarrie, N., Stock, J. M., Verdel, C., & Wernicke, B. P. (2003). Cenozoic evolution of Neotethys and implications for the causes of plate motions. *Geophysical Research Letters*, *30*(20), 2036. https://doi.org/10.1029/2003GL017992

Mishin, Y. A., Gerya, T. V., Burg, J. P., & Connolly, J. A. (2008). Dynamics of double subduction: Numerical modeling. *Physics of the Earth and Planetary Interiors*, *171*(1–4), 280–295. https://doi.org/10.1016/j.pepi.2008.06.012

Moix, P., Beccaletto, L., Kozur, H. W., Hochard, C., Rosselet, F., & Stampfli, G. M. (2008). A new classification of the Turkish terranes and sutures and its implication for the paleotectonic history of the region. *Tectonophysics*, *451*(1–4), 7–39. https://doi.org/10.1016/j.tecto.2007.11.044

Mueller, M. A., Licht, A., Campbell, C., Ocakoğlu, F., Akşit, G. G., Métais, G., et al. (2022). Sedimentary provenance from the evolving forearc-to-foreland Central Sakarya Basin, western Anatolia reveals multi-phase intercontinental collision. *Geochemistry, Geophysics, Geosystems*, *23*(3), e2021GC010232. https://doi.org/10.1029/2021GC010232

Mueller, M. A., Licht, A., Campbell, C., Ocakoğlu, F., Taylor, M. H., Burch, L., et al. (2019). Collision chronology along the İzmir-Ankara-Erzincan suture zone: Insights from the Sarıcakaya Basin, western Anatolia. *Tectonics*, *38*(10), 3652–3674. https://doi.org/10.1029/2019TC005683

Mulcahy, S. R., Vervoort, J. D., & Renne, P. R. (2014). Dating subduction-zone metamorphism with combined garnet and lawsonite Lu-Hf geochronology. *Journal of Metamorphic Geology*, *32*(5), 515–533. https://doi.org/10.1111/jmg.12092

Nikishin, A. M., Okay, A., Tüysüz, O., Demirer, A., Wannier, M., Amelin, N., & Petrov, E. (2015). The Black Sea basins structure and history: New model based on new deep penetration regional seismic data. Part 2: Tectonic history and paleogeography. *Marine and Petroleum Geology*, *59*, 656–670. https://doi.org/10.1016/j.marpetgeo.2014.08.018

Nikishin, A. M., Wannier, M., Alekseev, A. S., Almendinger, O. A., Fokin, P. A., Gabdullin, R. R., et al. (2017). Mesozoic to recent geological history of southern Crimea and the Eastern Black Sea region. *Geological Society, London, Special Publications*, *428*(1), 241–264. https://doi.org/10.1144/SP428.1

Nikishin, A. M., Ziegler, P. A., Bolotov, S. N., & Fokin, P. A. (2012). Late Palaeozoic to Cenozoic evolution of the Black Sea-Southern Eastern Europe Region: A view from the Russian Platform. *Turkish Journal of Earth Sciences*, *20*, 571–634. https://doi.org/10.3906/yer-1005-22

Noda, A. (2016). Forearc basins: Types, geometries, and relationships to subduction zone dynamics. *Bulletin*, *128*(5–6), 879–895. https://doi.org/10.1130/B31345.1

Ocakoğlu, F., Hakyemez, A., Açıkalın, S., Özkan Altıner, S., Büyükmeriç, Y., Licht, A., et al. (2018). Chronology of subduction and collision along the İzmir-Ankara suture in Western Anatolia: Records from the Central Sakarya Basin. *International Geology Review*, *61*(10), 1244–1269. https://doi.org/10.1080/00206814.2018.1507009TC5004

Okay, A., Tansel, İ., & Tüysüz, O. (2001). Obduction, subduction and collision as reflected in the Upper Cretaceous–Lower Eocene sedimentary record of western Turkey. *Geological Magazine*, *138*(2), 117–142. https://doi.org/10.1017/S0016756801005088

Okay, A. I. (1980a). Lawsonite zone blueschists and a sodic amphibole producing reaction in the Tavşanlı Region, Northwest Turkey. *Contributions to Mineralogy and Petrology*, *72*(3), 243–255. https://doi.org/10.1007/bf00376143

Okay, A. I. (1980b). Mineralogy, petrology and phase relations of Glaucophane–Lawsonite blueschists from the Tavşanlı region, northwest Turkey. *Contributions to Mineralogy and Petrology*, *72*(3), 243–255. https://doi.org/10.1007/bf00376143

Okay, A. I. (1982). Incipient blueschist metamorphism and metasomatism in the Tavşanlı Region, Northwest Turkey. *Contributions to Mineralogy and Petrology*, *79*(4), 361–367. https://doi.org/10.1007/bf01132065

Okay, A. I. (1984). Distribution and characteristics of the northwest Turkish blueschists. In J. E. Dixon & A. H. F. Robertson (Eds.), *The Geological Evolution of the Eastern Mediterranean* (Vol. 17, pp. 455–466). Geological Society of London Special Publication.

Okay, A. I. (1986). High-pressure/low-temperature metamorphic rocks of Turkey. *Geologic Society of America Memoirs*, *164*.

Okay, A. I. (2000). Was the Late Triassic orogeny in Turkey caused by the collision of an oceanic plateau? *Geological Society, London, Special Publications*, *173*(1), 25–41. https://doi.org/10.1144/GSL.SP.2000.173.01.02

Okay, A. I. (2002). Jadeite–chloritoid–glaucophane–lawsonite blueschists in north-west Turkey: Unusually high *P*/*T* ratios in continental crust. *Journal of Metamorphic Geology*, *20*(8), 757–768. https://doi.org/10.1046/j.1525-1314.2002.00402.x

Okay, A. I., Celal Şengör, A. M., & Görür, N. (1994). Kinematic history of the opening of the Black Sea and its effect on the surrounding regions. *Geology*, *22*(3), 267. https://doi.org/10.1130/0091-7613(1994)022<0267:khotoo>2.3.co;2

Okay, A. I., & Göncüoğlu, M. C. (2004). The Karakaya Complex: A review of data and concepts. *Turkish Journal of Earth Sciences*, *13*(2), 75–95.

Okay, A. I., Harris, N. B., & Kelley, S. P. (1998). Exhumation of blueschists along a Tethyan suture in northwest Turkey. *Tectonophysics*, *285*(3–4), 275–299. https://doi.org/10.1016/s0040-1951(97)00275-8

Okay, A. I., & Kelley, S. P. (1994). Tectonic setting, petrology and geochronology of jadeite+ glaucophane and chloritoid+ glaucophane schists from north-west Turkey. *Journal of Metamorphic Geology*, *12*(4), 455–466. https://doi.org/10.1111/j.1525-1314.1994.tb00035.x

Okay, A. I., Monod, O., & Monié, P. (2002). Triassic blueschists and eclogites from northwest Turkey: Vestiges of the Paleo-Tethyan subduction. *Lithos*, *64*(3–4), 155–178. https://doi.org/10.1016/S0024-4937(02)00200-1

Okay, A. I., & Nikishin, A. M. (2015). Tectonic evolution of the southern margin of Laurasia in the Black Sea region. *International Geology Review*, *57*(5–8), 1051–1076. https://doi.org/10.1080/00206814.2015.1010609

Okay, A. I., Satir, M., Maluski, H., Siyako, M., Monie, P., Metzger, R., & Akyüz, S. (1996). Paleo-and Neo-Tethyan events in northwestern Turkey: Geologic and geochronologic constraints. *World and Regional Geology*, 420e441.

Okay, A. I., Satır, M., & Shang, C. K. (2008). Ordovician metagranitoid from the Anatolide–Tauride Block, northwest Turkey: Geodynamic implications. *Terra Nova*, *20*(4), 280–288. https://doi.org/10.1111/j.1365-3121.2008.00818.x

Okay, A. I., Satir, M., & Siebel, W. (2006). Pre-Alpide Palaeozoic and Mesozoic orogenic events in the Eastern Mediterranean region. *Geological Society, London, Memoirs*, *32*(1), 389–405. https://doi.org/10.1144/GSL.MEM.2006.032.01.23

Okay, A. İ., Sunal, G., Sherlock, S., Altıner, D., Tüysüz, O., Kylander-Clark, A. R., & Aygül, M. (2013). Early Cretaceous sedimentation and orogeny on the active margin of Eurasia: Southern Central Pontides, Turkey. *Tectonics*, *32*(5), 1247–1271. https://doi.org/10.1002/tect.20077

Okay, A. I., Sunal, G., Sherlock, S., Kylander-Clark, A. R., & Özcan, E. (2020). İzmir-Ankara Suture as a Triassic to Cretaceous Plate Boundary—Data from Central Anatolia. *Tectonics*, *39*(5), e2019TC005849. https://doi.org/10.1029/2019TC005849

Okay, A. I., Tüysüz, O., Satır, M., Ozkan-Altiner, S., Altiner, D., Sherlock, S., & Eren, R. H. (2006). Cretaceous and Triassic subduction-accretion, high-pressure–low-temperature metamorphism, and continental growth in the Central Pontides, Turkey. *Geological Society of America Bulletin*, *118*(9–10), 1247–1269. https://doi.org/10.1130/B25938.1

Okay, A. I., & Tüysüz, O. (1999). Tethyan sutures of northern Turkey. *Geological Society, London, Special Publications*, *156*(1), 475–515. https://doi.org/10.1144/gsl.sp.1999.156.01.22

Okay, A. I., & Whitney, D. L. (2010). Blueschists, eclogites, ophiolites and suture zones in northwest Turkey: A review and a field excursion guide. *Ofioliti*, *35*(2), 131–172.

Okay, A. I., Zattin, M., & Cavazza, W. (2010). Apatite fission-track data for the Miocene Arabia-Eurasia collision. *Geology*, *38*(1), 35–38. https://doi.org/10.1130/G30234.1

Önen, A. P. (2003). Neotethyan ophiolitic rocks of the Anatolides of NW Turkey and comparison with Tauride ophiolites. *Journal of the Geological Society*, *160*(6), 947–962. https://doi.org/10.1144/0016-764902-125

Özkaptan, M., Gülyüz, E., Kaymakcı, N., & Langereis, C. G. (2021). Neogene restoration of geometry of the Neotethyan suture zone in Central Anatolia (Turkey). *International Geology Review*, *64*(21), 1–20. https://doi.org/10.1080/00206814.2021.2010133

Öztürk, Y. Y., Helvaci, C., & Satir, M. (2012). Geochemical and isotopic constraints on petrogenesis of the Beypazarı Granitoid, NW Ankara, western central Anatolia, Turkey. *Turkish Journal of Earth Sciences*, *21*(1), 53–77. https://doi.org/10.3906/yer-1006-1

Pearce, J. A., Lippard, S. J., & Roberts, S. (1984). Characteristics and tectonic significance of supra-subduction zone ophiolites. *Geological Society, London, Special Publications*, *16*(1), 77–94. https://doi.org/10.1144/gsl.sp.1984.016.01.06

Pickett, E. A., & Robertson, A. H. (2004). Significance of the volcanogenic Nilüfer Unit and related components of the Triassic Karakaya Complex for Tethyan subduction/accretion processes in NW Turkey. *Turkish Journal of Earth Sciences*, *13*(2), 97–143.

Plunder, A., Agard, P., Chopin, C., & Okay, A. I. (2013). Geodynamics of the Tavşanlı zone, western Turkey: Insights into subduction/obduction processes. *Tectonophysics*, *608*, 884–903. https://doi.org/10.1016/j.tecto.2013.07.028

Plunder, A., Agard, P., Chopin, C., Pourteau, A., & Okay, A. I. (2015). Accretion, underplating and exhumation along a subduction interface: From subduction initiation to continental subduction (Tavşanlı zone, W. Turkey). *Lithos*, *226*, 233–254. https://doi.org/10.1016/j.lithos.2015.01.007

Pourteau, A., Candan, O., & Oberhänsli, R. (2010). High-pressure metasediments in central Turkey: Constraints on the Neotethyan closure history. *Tectonics*, *29*(5). https://doi.org/10.1029/2009TC002650

Pourteau, A., Scherer, E. E., Schorn, S., Bast, R., Schmidt, A., & Ebert, L. (2019). Thermal evolution of an ancient subduction interface revealed by Lu–Hf garnet geochronology, Halilbağı Complex (Anatolia). *Geoscience Frontiers*, *10*(1), 127–148. https://doi.org/10.1016/j.gsf.2018.03.004

Pusok, A. E., & Stegman, D. R. (2019). Formation and stability of same-dip double subduction systems. *Journal of Geophysical Research: Solid Earth*, *124*(7), 7387–7412. https://doi.org/10.1029/2018JB017027

Robertson, A. (2004). Development of concepts concerning the genesis and emplacement of Tethyan ophiolites in the Eastern Mediterranean and Oman regions. *Earth-Science Reviews*, *66*(3–4), 331–387. https://doi.org/10.1016/j.earscirev.2004.01.005

Robertson, A. H. F., & Dixon, J. E. (1984). Introduction: Aspects of the geological evolution of the Eastern Mediterranean. *Geological Society, London, Special Publications*, *17*(1), 1–74. https://doi.org/10.1144/gsl.sp.1984.017.01.02

Robinson, A. G. (1997). AAPG Memoir 68: Regional and Petroleum Geology of the Black Sea and Surrounding Region. *Introduction: Tectonic Elements of the Black Sea and Surrounding Region (Chapter 1)*.

Rojay, B. (2013). Tectonic evolution of the Cretaceous Ankara ophiolitic mélange during the Late Cretaceous to pre-Miocene interval in Central Anatolia, Turkey. *Journal of Geodynamics*, *65*, 66–81. https://doi.org/10.1016/j.jog.2012.06.006

Rojay, B., Altıner, D., Altıner, S. Ö., Pırıl Önen, A., James, S., & Thirlwall, M. F. (2004). Geodynamic significance of the Cretaceous pillow basalts from North Anatolian Ophiolitic Mélange Belt (Central Anatolia, Turkey): Geochemical and paleontological constraints. *Geodinamica Acta*, *17*(5), 349–361. https://doi.org/10.3166/ga.17.349-361

Rolland, Y., Perincek, D., Kaymakci, N., Sosson, M., Barrier, E., & Avagyan, A. (2012). Evidence for ∼80–75 Ma subduction jump during Anatolide–Tauride–Armenian block accretion and∼ 48 Ma Arabia–Eurasia collision in Lesser Caucasus–East Anatolia. *Journal of Geodynamics*, *56*, 76–85. https://doi.org/10.1016/j.jog.2011.08.006

Şahin, M., Yaltırak, C., & Karacık, Z. (2019). A case study of compression to escape tectonic transition: Tectonic evolution of the Nallıhan Wedge and comparison with the Tercan Wedge (Eastern Mediterranean, Turkey). *Journal of Asian Earth Sciences*, *174*, 311–331. https://doi.org/10.1016/j.jseaes.2018.12.016

Sarıfakıoğlu, E., Dilek, Y., & Sevin, M. (2014). Jurassic–Paleogene intraoceanic magmatic evolution of the Ankara Mélange, north-central Anatolia, Turkey. *Solid Earth*, *5*(1), 77–108. https://doi.org/10.5194/se-5-77-2014

Sarıfakıoğlu, E., Dilek, Y., Sevin, M., & Sorkhabi, R. (2017). *New synthesis of the Izmir-Ankara-Erzincan suture zone and the Ankara mélange in northern Anatolia based on new geochemical and geochronological constraints. Tectonic evolution, collision, and seismicity of Southwest Asia: In honor of Manuel Berberian's forty-five years of research contributions* (p. 525). Geological Society of America Special Paper. https://doi.org/10.1130/2017.2525(19)

Sarıfakıoğlu, E., Özen, H., Çolakoğlu, A., & Sayak, H. (2010). Petrology, mineral chemistry, and tectonomagmatic evolution of Late Cretaceous suprasubduction-zone ophiolites in the İzmir–Ankara–Erzincan suture zone, Turkey. *International Geology Review*, *52*(2–3), 187–222. https://doi.org/10.1080/00206810902818479

Sarıfakıoğlu, E., Özen, H., & Winchester, J. A. (2009). Whole rock and mineral chemistry of ultramafic–mafic cumulates from the Orhaneli (Bursa) ophiolite, NW Anatolia. *Turkish Journal of Earth Science*, *18*, 55–83. https://doi.org/10.3906/yer-0806-8

Scherer, E., Münker, C., & Mezger, K. (2001). Calibration of the lutetium-hafnium clock. *Scienc*e, *293*(5530), 683–687. https://doi.org/10.1126/science.1061372

Seaton, N. C. A., Teyssier, C., Whitney, D. L., & Heizler, M. T. (2014). Quartz and calcite microfabric transitions in a pressure and temperature gradient, Sivrihisar, Turkey. *Geodinamica Acta*, *26*(3–4), 191–206. https://doi.org/10.1080/09853111.2013.858952

Seaton, N. C. A., Whitney, D. L., Teyssier, C., Toraman, E., & Heizler, M. T. (2009). Recrystallization of high-pressure marble (Sivrihisar, Turkey). *Tectonophysics*, *479*(3–4), 241–253. https://doi.org/10.1016/j.tecto.2009.08.015

Şengör, A. C., & Yilmaz, Y. (1981). Tethyan evolution of Turkey: A plate tectonic approach. *Tectonophysics*, *75*(3–4), 181–241. https://doi.org/10.1016/0040-1951(81)90275-4

Şengör, A. M. C. (1987). Tectonics of the Tethysides: Orogenic collage development in a collisional setting. *Annual Review of Earth and Planetary Sciences*, *15*(1), 213–244. https://doi.org/10.1146/annurev.ea.15.050187.001241

Şengör, A. M. C., Yılmaz, Y., & Sungurlu, O. (1984). Tectonics of the Mediterranean Cimmerides: Nature and evolution of the western termination of Palaeo-Tethys. *Geological Society, London, Special Publications*, *17*(1), 77–112. https://doi.org/10.1144/gsl.sp.1984.017.01.04

Sherlock, S., & Kelley, S. (2002). Excess argon evolution in HP–LT rocks: A UVLAMP study of phengite and K-free minerals, NW Turkey. *Chemical Geology*, *182*(2–4), 619–636. https://doi.org/10.1016/S0009-2541(01)00345-X

Sherlock, S., Kelley, S., Inger, S., Harris, N., & Okay, A. I. (1999). ^{40}Ar–^{39}Ar and Rb–Sr geochronology of high-pressure metamorphism and exhumation history of the Tavsanli Zone, NW Turkey. *Contributions to Mineralogy and Petrology*, *137*(1–2), 46–58.

Söderlund, U., Patchett, P. J., Vervoort, J. D., & Isachsen, C. E. (2004). The ^{176}Lu decay constant determined by Lu–Hf and U–Pb isotope systematics of Precambrian mafic intrusions. *Earth and Planetary Science Letters*, *219*(3–4), 311–324. https://doi.org/10.1016/S0012-821X(04)00012-3

Speciale, P. A., Catlos, E. J., Yıldız, G. O., Shin, T. A., & Black, K. N. (2012). Zircon ages from the Beypazarı granitoid pluton (north central Turkey): Tectonic implications. *Geodinamica Acta*, *25*(3–4), 162–182. https://doi.org/10.1080/09853111.2013.858955

Stampfli, G. M. (2000). Tethyan oceans. *Geological Society of London Special Publications*, *173*(1), 1–23. https://doi.org/10.1144/GSL.SP.2000.173

Stampfli, G. M., Borel, G. D., Marchant, R., & Mosar, J. (2002). Western Alps geological constraints on western Tethyan reconstructions. *Journal of the Virtual Explorer*, *8*, 77. https://doi.org/10.1016/S0012-821X(01)00588-X

Stampfli, G. M., & Hochard, C. (2009). Plate tectonics of the Alpine realm. *Geological Society of London, Special Publications*, *327*(1), 89–111. https://doi.org/10.1144/SP327.6

Sundell, K., Saylor, J. E., & Pecha, M. (2019). Provenance and recycling of detrital zircons from Cenozoic Altiplano strata and the crustal evolution of western South America from combined U-Pb and Lu-Hf isotopic analysis. In *Andean Tectonics* (pp. 363–397). Elsevier. https://doi.org/10.1016/B978-0-12-816009-1.00014-9

Sundell, K. E., George, S. W., Carrapa, B., Gehrels, G. E., Ducea, M. N., Saylor, J. E., & Pepper, M. (2022). Crustal thickening of the northern Central Andean Plateau inferred from trace elements in zircon. *Geophysical Research Letters*, *49*(3), e2021GL096443. https://doi.org/10.1029/2021GL096443

Tekin, U. K., Göncüoğlu, M. C., & Turhan, N. (2002). First evidence of Late Carnian radiolarians from the Izmir–Ankara suture complex, central Sakarya, Turkey: Implications for the opening age of the Izmir–Ankara branch of Neo-Tethys. *Geobios*, *35*(1), 127–135. https://doi.org/10.1016/S0016-6995(02)00015-3

Topuz, G., Altherr, R., Schwarz, W. H., Dokuz, A., & Meyer, H. P. (2007). Variscan amphibolite-facies rocks from the Kurtoğlu metamorphic complex (Gümüşhane area, Eastern Pontides, Turkey). *International Journal of Earth Sciences*, *96*(5), 861–873. https://doi.org/10.1007/s00531-006-0138-y

Topuz, G., Altherr, R., Siebel, W., Schwarz, W. H., Zack, T., Hasözbek, A., et al. (2010). Carboniferous high-potassium I-type granitoid magmatism in the Eastern Pontides: The Gümüşhane pluton (NE Turkey). *Lithos*, *116*(1–2), 92–110. https://doi.org/10.1016/j.lithos.2010.01.003

Topuz, G., Candan, O., Okay, A. I., von Quadt, A., Othman, M., Zack, T., & Wang, J. (2020). Silurian anorogenic basic and acidic magmatism in Northwest Turkey: Implications for the opening of the Paleo-Tethys. *Lithos*, *356*, 105302. https://doi.org/10.1016/j.lithos.2019.105302

Topuz, G., Hegner, E., Homam, S. M., Ackerman, L., Pfänder, J. A., & Karimi, H. (2018). Geochemical and geochronological evidence for a Middle Permian oceanic plateau fragment in the Paleo-Tethyan suture zone of NE Iran. *Contributions to Mineralogy and Petrology*, *173*(10), 1–23. https://doi.org/10.1007/s00410-018-1506-x

Topuz, G., Okay, A. I., Altherr, R., Meyer, H. P., & Nasdala, L. (2006). Partial high-pressure aragonitization of micritic limestones in an accretionary complex, Tavşanlı Zone, NW Turkey. *Journal of Metamorphic Geology*, *24*(7), 603–613. https://doi.org/10.1111/j.1525-1314.2006.00657.x

Tüysüz, O. (1999). Geology of the Cretaceous sedimentary basins of the Western Pontides. *Geological Journal*, *34*(1-2), 75–93. https://doi.org/10.1002/(sici)1099-1034(199901/06)34:1/2<75::aid-gj815>3.0.co;2-s

Tüysüz, O., & Tekin, U. K. (2007). Timing of imbrication of an active continental margin facing the northern branch of Neotethys, Kargı Massif, northern Turkey. *Cretaceous Research*, *28*(5), 754–764. https://doi.org/10.1016/j.cretres.2006.11.006

Ustaömer, A. P., Mundil, R., & Renne, P. R. (2005). U/Pb and Pb/Pb zircon ages for arc-related intrusions of the Bolu Massif (W Pontides, NW Turkey): Evidence for Late Precambrian (Cadomian) age. *Terra Nova*, *17*(3), 215–223. https://doi.org/10.1111/j.1365-3121.2005.00594.x

Ustaömer, T., Robertson, A. H. F., Ustaömer, P. A., Gerdes, A., & Peytcheva, I. (2013). Constraints on Variscan and Cimmerian magmatism and metamorphism in the Pontides (Yusufeli-Artvin area), NE Turkey from U-Pb dating and granite geochemistry. *Geological Society, London, Special Publications*, *372*(1), 49–74. https://doi.org/10.1144/SP372.13

Ustaömer, T., Ustaömer, P. A., Robertson, A. H., & Gerdes, A. (2016). Implications of U–Pb and Lu–Hf isotopic analysis of detrital zircons for the depositional age, provenance and tectonic setting of the Permian–Triassic Palaeotethyan Karakaya Complex, NW Turkey. *International Journal of Earth Sciences*, *105*(1), 7–38. https://doi.org/10.1007/s00531-015-1225-8

Ustaömer, T., Ustaömer, P. A., Robertson, A. H., & Gerdes, A. (2020). U-Pb-Hf isotopic data from detrital zircons in late Carboniferous and Mid-Late Triassic sandstones, and also Carboniferous granites from the Tauride and Anatolide continental units in S Turkey: Implications for Tethyan palaeogeography. *International Geology Review*, *62*(9), 1159–1186. https://doi.org/10.1080/00206814.2019.1636415

van der Kaaden, G. (1966). The significance and distribution of glaucophane rocks in Turkey. *Bulletin. Mineral Research and Exploration Institute*, *67*, 37–67.

van Hinsbergen, D. J., Maffione, M., Plunder, A., Kaymakcı, N., Ganerød, M., Hendriks, B. W., et al. (2016). Tectonic evolution and paleogeography of the Kırşehir Block and the Central Anatolian Ophiolites, Turkey. *Tectonics*, *35*(4), 983–1014. https://doi.org/10.1002/2015tc004018

van Hinsbergen, D. J., Torsvik, T. H., Schmid, S. M., Maţenco, L. C., Maffione, M., Vissers, R. L., et al. (2020). Orogenic architecture of the Mediterranean region and kinematic reconstruction of its tectonic evolution since the Triassic. *Gondwana Research*, *81*, 79–229. https://doi.org/10.1016/j.gr.2019.07.009

Vermeesch, P., Resentini, A., & Garzanti, E. (2016). An R package for statistical provenance analysis. *Sedimentary Geology*, *336*, 14–25. https://doi.org/10.1016/j.sedgeo.2016.01.009

Westerweel, J., Roperch, P., Licht, A., Dupont-Nivet, G., Win, Z., Poblete, F., et al. (2019). Burma Terrane part of the Trans-Tethyan arc during collision with India according to palaeomagnetic data. *Nature Geoscience*, *12*(10), 863–868. https://doi.org/10.1038/s41561-019-0443-2

Wolfgring, E., Wagreich, M., Dinarès-Turell, J., Yilmaz, I. O., & Böhm, K. (2017). Plankton biostratigraphy and magnetostratigraphy of the Santonian–Campanian boundary interval in the Mudurnu–Göynük Basin, northwestern Turkey. *Cretaceous Research*, *87*, 296–311. https://doi.org/10.1016/j.cretres.2017.07.006

Yalınız, M. K. (2008). A geochemical attempt to distinguish forearc and back arc ophiolites from the "supra-subduction" central Anatolian ophiolites (Turkey) by comparison with modern oceanic analogues. *Ofioliti*, *33*(2), 119–129. https://doi.org/10.4454/ofioliti.v33i2.363

Yaliniz, M. K., Floyd, P. A., & Göncüoğlu, M. C. (1996). Supra-subduction zone ophiolites of Central Anatolia: Geochemical evidence from the Sarikaraman ophiolite, Aksaray, Turkey. *Mineralogical Magazine*, *60*(402), 697–710. https://doi.org/10.1180/minmag.1996.060.402.01

Yalınız, M. K., & Göncüoğlu, M. C. (1998). General geological characteristics and distribution of the Central Anatolian Ophiolites. *Yerbilimleri*(20), 19–30.

Yaliniz, M. K., Göncüoğlu, M. C., & Özkan-Altiner, S. (2000). Formation and emplacement ages of the SSZ-type Neotethyan ophiolites in central Anatolia, Turkey: Palaeotectonic implications. *Geological Journal*, *35*(2), 53–68. https://doi.org/10.1002/1099-1034(200004/06)35:2<53::AID-GJ837>3.0.CO;2-6

Yilmaz, A., Adamia, S., Chabukiani, A., Chkhotua, T., Erdoğan, K., Tuzcu, S., & KarabiyikoGlu, M. (2000). Structural correlation of the southern Transcaucasus (Georgia)-eastern Pontides (Turkey). *Geological Society, London, Special Publications*, *173*(1), 171–182. https://doi.org/10.1144/gsl.sp.2000.173.01.08

Yilmaz, I. O., Altiner, D., & Ocakoglu, F. (2016). Upper Jurassic–Lower Cretaceous depositional environments and evolution of the Bilecik (Sakarya Zone) and Tauride carbonate platforms, Turkey. *Palaeogeography, Palaeoclimatology, Palaeoecology*, *449*, 321–340. https://doi.org/10.1016/j.palaeo.2016.02.028

Yin, A., & Harrison, T. M. (2000). Geologic evolution of the Himalayan-Tibetan orogen. *Annual Review of Earth and Planetary Sciences*, *28*(1), 211–280. https://doi.org/10.1146/annurev.earth.28.1.211